Summer 8-17-2018

Transcriptional regulation of icaADBC by IcaR and TcaR in Staphylococcus epidermidis

Tramy Hoang
University of Nebraska Medical Center

Transcriptional regulation of *icaADBC* by IcaR and TcaR in *Staphylococcus epidermidis*

By
Tra-My N. Hoang

A DISSERTATION

Presented to the Faculty of
the University of Nebraska Graduate College
in Partial Fulfillment of the Requirements
for the Degree of Doctor of Philosophy

Pathology and Microbiology

Under the Supervision of Professor Paul D. Fey

University of Nebraska Medical Center
Omaha, Nebraska

August 2018

Supervisory Committee:

Kenneth Bayles, Ph.D.
Steven Carson, Ph.D.
Vinai Chittezham Thomas, Ph.D.

Acknowledgements

This dissertation would not be possible without the support of many people. First, Paul Fey. I cannot thank you enough for all you have done and all the patience and wisdom you have shown me. You have taught me not only what good science is but also how to be a good scientist, teacher, and person. Thanks for all the lessons and good times.

Thank you to my committee. I appreciate every minute that you have spent providing me with input and advice. Additionally, thanks for opening your labs up to me when I needed a piece of equipment, a place to run an experiment or just seeking your expertise.

And to all the people I have had the pleasure of working with. The Bayles and Thomas labs: thank you for being so generous with your time when I need help and advice. Especially Jennifer: thank you for never hesitating to come to my rescue and for being such a good friend. The past and present members of the Fey lab: you have taken the time to teach me, troubleshoot with me, commiserate with me, laugh with me, eat with me, and explored new places with me. I am so very lucky to have crossed paths with you and am grateful for your friendships.

To my parents. I would not be the person I am nor would I have gotten to where I am without you. You have shown me that nothing comes without hard work and perseverance. Thank you for all the sacrifices you have made so I can pursue my dreams. I hope I have made you proud. Huey and Duy, I love being your sister and am so proud of the people you have become. Just know that I will forever be your big sister and will always be there for you. Thương cả nhà nhiều lắm.

Last, but not least, my husband Brad. Thank you for being my best friend. Your patience, optimism, intellect, ambition, and own hard work have been sources of motivation and inspiration to me. Here's to our future and to all the adventures that we'll embark on. There's no one else I'd rather do this with.

Regulation of *icaADBC* by IcaR and TcaR in *Staphylococcus epidermidis*

Tra-My N. Hoang, Ph.D.

University of Nebraska, 2018

Advisor: Paul D. Fey, Ph.D.

Biofilm formation is the primary virulence factor in *Staphylococcus epidermidis.* Polysaccharide intercellular adhesin (PIA) is an adhesive molecule and a significant component of the biofilm matrix. It is synthesized by the products of the *icaADBC* operon whose regulation has been shown to involve environmental factors as well as many transcriptional regulators. Of these regulators, we explored the function of the repressors IcaR and TcaR and their roles in directly influencing *icaADBC* transcription and PIA synthesis. Based on previous observations that *icaADBC* positive clinical isolates of *S. epidermidis* are highly variable in PIA synthesis and biofilm formation, our goal was to further investigate why this may be. We generated *icaR* and *tcaR* mutations in *S. epidermidis* strain 1457, a high PIA producing strain, and CSF41498, a low and inducible PIA producing strain. We observed that *icaADBC* is primarily regulated by TcaR in 1457 and by IcaR in CSF41498 and this may be due to *icaR* being expressed at lower levels in 1457, leading to de-repression of *icaADBC*. DNase I footprinting results confirmed that TcaR binds to multiple sequences in the *icaR-icaA* intergenic region, including the *ica* and *icaR* promoters, providing evidence that TcaR can repress both *icaADBC* and *icaR* transcription. Finally, we generated mutants in CSF41498 exhibiting high PIA synthesis as well as mutants in 1457 that were no longer able to synthesize high levels of PIA. Sequencing of these mutants provided insight into genes with potential functions in regulating *icaADBC*. Overall, our data demonstrate the complexity with which *icaADBC* is regulated, especially in regards to IcaR and TcaR, and that *icaADBC* regulation is strain specific.

.

TABLE OF CONTENTS

TABLES AND FIGURES

CHAPTER 1

Introduction

Staphylococcus epidermidis is often isolated from infections in humans and is the most commonly associated bacteria isolated from infected medical implants (1). The genomes of *S. aureus* and *S. epidermidis* contain only subtle differences, however the former is a major human pathogen while the latter is generally considered a skin commensal. Upon analysis of the genomes, it was found that nonsyntenic genes found in *S. aureus* (and not *S. epidermidis*) encoding for enterotoxins, exotoxins, leukocidins, and leukotoxins most likely account for the difference in pathogenicity (2-4). However, the ability of S. epidermidis to form biofilms gives it a significant advantage within a host.

BIOFILMS

Biofilms are defined as an aggregation of bacteria formed on the surface of host tissue or non-biological surfaces such as medical implants. The formation of biofilms allows bacteria to become more resistant to host immune responses as well as antibiotics. In fact, bacteria within a biofilm can be up to 1000-fold more resistant to antibiotics than those grown planktonically (5, 6)). Biofilm infections are difficult to treat and most often require removal of the infected device, followed by antibiotic therapy and replacement of the device (7, 8).

Though not clearly defined, biofilm formation is generally described as occurring in four stages beginning with attachment. During this stage, adhesion to foreign surfaces occurs via nonspecific and hydrophobic interactions mediated by proteins such as AtlE (9). Additionally, microbial surface components recognizing adhesive matrix molecules (MSCRAMMs), including SdrG, SdrF, Embp, and SesC, have been shown to bind host serum proteins that rapidly coat foreign surfaces (10-18) . Next, multiplication and maturation of the biofilm occurs via synthesis of an extracellular matrix consisting of exopolysaccharides, teichoic acids, proteins and extracellular DNA (eDNA) (19-24). This matrix allows for adherence of the cells to each other as well as the attachment surface. During this stage, channels and other structures are formed that allow for movement of nutrients and waste

throughout the biofilm (25, 26). Moormeier et al. have also identified an additional stage of biofilm formation whereby, after formation of a confluent "lawn," a subpopulation of cells leaves the biofilm allowing the remaining cells to form a mature biofilm tower. This "exodus" event was found to be nuclease dependent (27). Finally, the dissemination stage is when detachment and dispersion of the biofilm occurs, resulting in infection of distal sites via the lymphatic system or the bloodstream (1, 25, 26, 28, 29). Proteases, nucleases, and phenol-soluble modulins (PSMs) have been shown to be involved in this stage (30-36).

POLYSACCHARIDE INTERCELLULAR ADHESIN

Polysaccharide intercellular adhesin (PIA), or PNAG (poly-β (1,6)-*N*-acetylglucosamine), was originally identified in *S. epidermidis* and *S. aureus* and has since been shown to be produced by Gram-negative bacteria as well as some eukaryotes (37-44). PIA has been well described in the literature as an important biofilm component with function in accumulation (23, 43, 45-64). *S. epidermidis* strains expressing PIA have more robust biofilm structures compared to strains defective in PIA synthesis (48).

PIA is a β-1,6-linked poly-*N*-acetyl-D-glucosamine (PNAG) polymer synthesized by the products of the *icaADBC* operon (23, 55, 65) . IcaA is an *N*-acetyl-glucosaminyltransferase responsible for producing PNAG (50). Although IcaD is thought to enhance, and is essential, for IcaA activity, the exact function is not known (49). IcaB is an extracellular protein responsible for partial deacetylation of PIA, allowing for association with the cell surface and adherence of the cell to various surfaces (53, 66, 67). Finally, the function of IcaC is predicted to export mature PNAG polymers (50). However, it was recently proposed that IcaC may function as an *O*-succinyltransferase due to sequence similarity to a family of acetyltransferases (68).

ROLE OF PIA IN PATHOGENICITY

In *S. epidermidis*, the ability to form biofilms is the primary virulence factor and synthesis of PIA is an important method by which *S. epidermidis* forms biofilms (64, 69, 70). Commensal strains do not carry the the *icaADBC* operon as often as clinical isolates (29, 58, 64, 69, 71-73). 45% of *S. epidermidis* hospital-associated infections are *ica*-positive as well as 80% of *S. epidermidis* strains isolated from prosthetic joint infections (45, 58). In fact, PIA is essential for facilitating adhesion to medical implants (74). *In vivo*, PIA has been shown to be important in a foreign-body-associated infection model in rats as well as a subcutaneous foreign body infection model in mice (59-61).

While the innate immune system can respond to *S. epidermidis* infections by activating the complement system, (75, 76), the presence of PIA, in both planktonic and biofilm states, have been shown to protect cells from phagocytosis and killing by polymorphonuclear neutrophils (PMNs) (63, 77-79). A different study found that, when using anti-PIA IgG, cells in a biofilm exhibit less phagocytic killing compared to planktonically grown cells (67, 80, 81). Furthermore, Cerca et al. demonstrated that this is true even when biofilms were dispersed, suggesting that the biofilm matrix itself does not provide protection against antibody-mediated phagocytosis and killing (82). Finally, PIA has been shown to protect cells against human antimicrobial peptides and *S. epidermidis* clinical isolates carrying *icaADBC* were resistant to multiple classes of antibiotics (45, 83). These data suggest that PIA has function to protect *S. epidermidis* from attack by the host immune system, as well as against antibiotics.

REGULATION OF *icaADBC*

The *icaADBC* operon is tightly regulated by numerous environmental and transcriptional regulators (Figure 1.2). Anaerobic growth, certain antibiotics, and environmental stresses can influence expression of *ica,* and thus PIA synthesis (84-86). Multiple studies have found that the presence of NaCl (4-10%) or ethanol (4%) induces

expression of *icaADBC* (87, 88). Additionally, shear stress has been found to be involved in regulation of the *ica* operon. Weaver et al. has reported that, in PIA-positive strains, biofilms grown under high shear flow contain streamers and are more web-like compared to the homogenous biofilms grown under low shear. Additionally, these investigators found that an *ica*-positive strain was unable to synthesize PIA unless in the presence of shear flow (89). Furthermore, a higher percentage of *S. epidermidis* strains isolated from high shear environments (such as intravascular catheters) carry *icaADBC* compared to those from low shear environments (such as cerebral spinal fluid shunts). Finally, transcription of *icaA* is significantly higher in biofilms grown under high flow compared to low flow (48, 90) suggesting that PIA is advantageous for colonization and formation of biofilm in high shear environments.

Metabolism. The regulation of PIA also depends on the metabolic state of the cell. During nutrient rich conditions, the TCA cycle is inactive and the intracellular concentration of glucose-6-phosphate is high, resulting in overflow metabolism channeling carbon towards PIA synthesis (62, 91). In addition, TCA cycle activity regulates *icaADBC* transcription, likely indirectly via regulators responding to the metabolic status of the cells (91). Sadykov et al. has shown that inactivation of the TCA cycle leads to increased *icaR, sigB,* and *sarA* mRNA levels suggesting that at least one of these known *icaADBC* regulators respond to changes in the TCA cycle to regulate *icaADBC* (91). Another possible regulator is catabolite control protein A (CcpA) which has been shown to be a minor activator of PIA synthesis when the TCA cycle is inactive (91, 92). Furthermore, CcpA has been shown to both regulate and is regulated by TCA cycle activity (93-96). However, further studies are required to confirm whether CcpA is in fact regulating *icaADBC* in response to the TCA cycle.

σ^B. The alternative sigma factor σ^B regulates stress response in low GC content Gram-positive bacteria, including staphylococci (97-99). σ^B regulates cellular responses to stresses

including heat, high osmolarity, extreme pH, ethanol, oxidizing agents, and shear stress (100, 101). Within staphylococci, the σ^B operon consists of *rsbU, rsbV, rsbW,* and *sigB*. Under normal conditions, RsbW binds σ^B. Under stressful conditions, RsbU dephosphorylates RsbV, allowing RsbV to bind RsbW and releasing σ^B from the complex (97, 102). Microarray studies in *S. aureus* have shown that the σ^B regulon is vast, consisting of about 250 genes (103, 104).

Considering the role of environmental factors in biofilm formation and PIA synthesis, it is not surprising that σ^B positively regulates *icaADBC.* A mutant defective in σ^B function has decreased cell aggregation and PIA synthesis, most likely due to increased *icaR* transcription and decreased *icaADBC* transcription (84, 105). However, no recognition sequence for σ^B was found in the *icaR-icaADBC* intergenic region, suggesting that this regulation is indirect and involves additional, yet unidentified, factors (46, 106).

IcaR. Upstream of the *ica* operon is the divergently transcribed *icaR* gene, a member of the TetR family of transcriptional regulators encoding a transcriptional repressor of *icaADBC* (88, 107). Like other members of this family, IcaR regulates transcription by binding to the promoter region. Specifically, electrophoretic mobility shift assay (EMSA) and computer modeling have identified a 22-24 bp sequence in the *ica* promoter region where IcaR is proposed to bind (108). Structural studies have shown that IcaR binds as two homodimers to DNA. Moreover, this sequence overlaps with the *icaADBC* transcriptional start site which is located at the adenosine 29 nucleotides upstream of the *icaA* start codon (50) (Figure 1.1).

IcaR does not regulate its own expression (88, 109) and has been shown to be regulated by several regulators (discussed below), including σ^B. When σ^B is inactivated, *icaR* transcription is increased and *icaA* transcription is abolished, indicating that σ^B regulation of *icaADBC* involves repression of *icaR.* Moreover, the presence of NaCl and ethanol can repress

icaR although repression of *icaR* by NaCl involves σ^B while repression by ethanol is σ^B-independent (84, 87, 88, 105).

TcaR. TcaR (teicoplanin-associated locus regulator) belongs to the family of MarR transcriptional regulators whose function involves teicoplanin and methicillin resistance (110). Like other members of the MarR family, TcaR binds to DNA as a dimer and this interaction can be inhibited by antibiotics, including gentamicin, streptomycin, and kanamycin (111). TcaR has been shown, in *S. aureus,* to regulate expression of the cell wall-anchored proteins Spa and SasF, as well as SarS, a regulator of virulence factors, as well as IcaADBC (110, 112). TcaR has been reported to have three putative binding sequences in the *icaR-icaA* intergenic region (Figure 1.1), showing that TcaR functions as a direct repressor (111, 113). Further knowledge regarding TcaR and its role in regulating *icaADBC* and PIA synthesis is limited.

SarA. The staphylococcal accessory regulator SarA, regulates a large number of virulence factors including the accessory gene regulator *agr,* a quorum sensing system important for colonization (114-116). In addition, SarA has been shown to be necessary for *ica* expression and PIA synthesis in both *S. aureus* and *S. epidermidis* (109, 117-120)). Of the three *sarA* promoters,

one has been shown to be σ^B-dependent. However, it has been demonstrated that σ^B-dependent regulation of *sarA* does not affect PIA synthesis, indicating that σ^B and SarA regulation of *icaADBC* is independent of each other (106, 121).

Other *icaADBC* regulators

Rbf. Rbf (regulator of biofilm formation) regulates biofilm by activating *sarX*, leading to repression of *icaR* and de-repression of *icaADBC* in *S. aureus* (122, 123). However, in *S. epidermidis,* Rbf regulates *icaADBC* by repressing *sarR* and *sarX*, which encode for a repressor and an activator of *icaADBC*, respectively. Rbf regulation of *icaADBC* in *S. epidermidis* occurs independent of IcaR (124, 125).

SrrAB. Staphylococcal respiratory response is a two-component signal transduction system that functions during anaerobic conditions to regulate genes involved in virulence (126). Deletion of *srrAB* in *S. epidermidis* causes impaired biofilm formation. In this same study, microarray results showed that transcription of *icaR* and *icaA* were decreased in a *srrAB* mutant in microaerobic conditions. However, in oxic conditions, *icaR* is upregulated and *icaADBC* is downregulated in the *srrAB* mutant (127). These data suggest that SrrAB regulates *icaR* and *icaADBC* in an oxygen-dependent manner.

ArlRS. In *S. aureus,* the two-component signal transduction system ArlRS is a global regulator of virulence genes, including capsule formation, biofilm formation, protein A, and α-toxin (128, 129). In *S. epidermidis*, ArlR was shown to bind directly to the *icaR-icaA* intergenic region, resulting in repression of *icaR* and de-repression of *icaADBC* (130).

CodY. In an effort to understand CodY regulation of virulence factors in *S. aureus,* Majerczyk et al. found that *icaADBC* is repressed by CodY during exponential phase, leading to

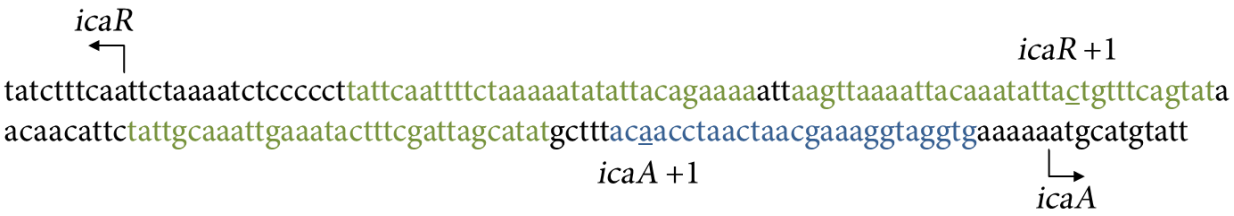

Figure 1.1 Sequence of the *icaR-icaA* intergenic region. IcaR binding site is in blue, the three proposed TcaR binding sites are in green. Transcriptional start sites for *icaR* and *icaA* are marked with +1 and underlined.

decreased PIA synthesis. Furthermore, transcription of *icaR* was not altered in the *codY* mutant, indicating that CodY regulation of *icaADBC* occurs independently of IcaR (131). While a canonical CodY box was identified in *icaB*, it remains to be determined whether CodY repression of *icaADBC* is direct or indirect (132). It is unclear whether CodY plays a similar role in *S. epidermidis.*

AI-2. Autoinducer-2, synthesized by LuxS is a family of small, diffusible molecules with function in quorum-sensing (133). In *S. aureus*, AI-2 indirectly activates *icaR* by repressing *rbf,* leading to repression of *icaADBC* and biofilm formation (123, 134, 135). In contrast, in *S. epidermidis,* AI-2 has been shown to upregulate *icaADBC* expression via repression of *icaR* (136).

Spx. Spx is a global regulator that functions by interacting with the α subunit of RNA polymerase and tightly regulated, post-transcriptionally, by the protease ClpP (137, 138). A *spx* mutant was shown to exhibit increased biofilm formation as a result of decreased *icaR* transcription and increased *icaADBC* transcription (138).

RELEVANCE OF PIA

While PIA has been shown to be important for biofilm formation (as discussed above), many studies have reported that *icaADBC* is not present in all *S. epidermidis* strains. In fact, less than half of clinical isolates carry this operon (45, 64, 72, 90, 139-141), suggesting that the ability to synthesize PIA is not always necessary for causing disease. Multiple investigators have also shown that the *ica* operon can be easily lost within a population. For example, Brooks and Jefferson found that a constitutive PIA hyper-producing mutant of *S. aureus* easily gained mutations resulting in loss of PIA production. One such mutation, a tetranucleotide repeat indel in *icaC*, occurred most often and can also be found in clinical isolates of *S. aureus* (142). Ziebuhr et al.

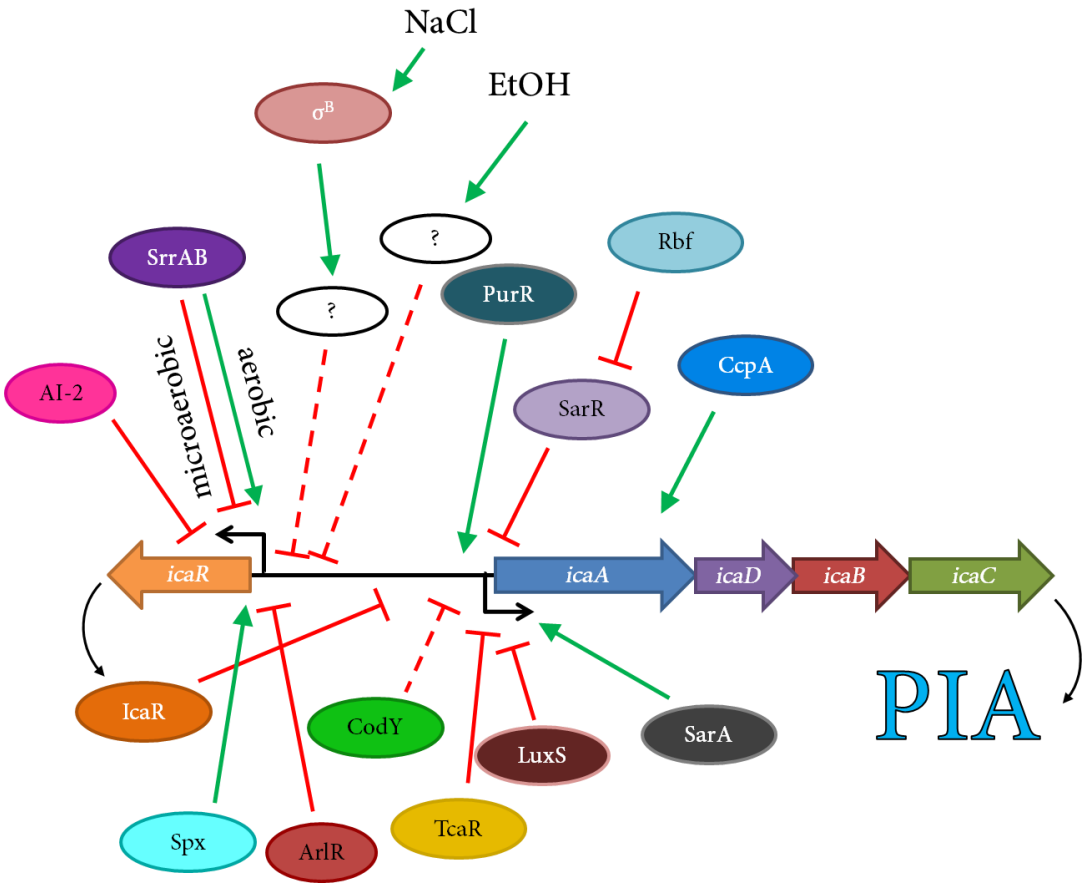

Figure 1.2 Regulators of *icaR* and *icaADBC*. Schematic of *icaR* and *icaADBC* with known regulators (ovals). Red hammerheads indicate repression, green arrows indicate activation, and dashed line indicates regulation could be direct or indirect.

reported that 30% of biofilm negative variants they studied were the result of movement of the mobile genetic element IS256 into *icaADBC*, most preferably *icaC* (143). This same study also showed that PIA negative mutants occurred at a rate of about 10^{-5} which is in agreement with other reports that the ability to synthesize PIA is easily lost (64, 144, 145). These data suggest that the presence of the *ica* operon, and the ability to synthesize PIA, is not essential for virulence. While numerous studies have reported the importance of PIA synthesis, it is not well understood when and why it would be advantageous to lose this ability. However, it is clear that there are certain conditions in which it is not beneficial to make PIA. In a study performed by Rogers et al., the forearms of healthy human participants were inoculated with either *S. epidermidis* wild-type or the *icaA* mutant. After 10 days, it was found that the mutant survived better on the skin than wild-type. Similarly, other studies have reported that, compared to *S. epidermidis* isolates that cause disease, the *ica* operon is not as prevalent in commensal strains of healthy individuals (64, 72, 73).

Additionally, the presence of the *ica* operon does not always correlate with PIA synthesis (58, 64, 90, 146-148). In agreement with this, Schaeffer et al. analyzed a very large collection (105) of *S. epidermidis* clinical isolates and found that amongst strains that are *ica*-positive (36), only 24 (~67%) actually synthesize PIA (90) suggesting that *S. epidermidis* is tightly regulating PIA. This provides further evidence that synthesis of PIA is not always favorable.

Investigations into PIA has shown that it is a significant component of biofilm formation and plays a major role in the ability of *S. epidermidis* to interact with the host immune system and cause disease. However, there is also evidence showing that *icaADBC* can be detrimental to bacterial fitness in certain environments. For this reason, it is important for *S. epidermidis* to carefully regulate *icaADBC* and control when PIA is synthesized. Since IcaR and TcaR have been shown to directly regulate *icaADBC,* we hypothesize that the variation in

icaADBC expression and PIA synthesis in *S. epidermidis* is due to the absence of *icaR* or *tcar* expression.

CHAPTER 2

Materials and methods

Bacterial culture conditions. Bacterial strains and plasmids are listed in Table 2.1. *Escherichia coli* was grown in Luria-Bertani broth (LB) (Becton Dickinson Difco; Franklin Lakes, NJ) and Staphylococcal strains were cultured using Tryptic Soy Broth (TSB) (Becton Dickinson Difco). LB and TSB agar plates (LBA, TSA respectively) were prepared by autoclaving LB or TSB with 0.5% (w/v) agar (Becton Dickinson Difco) and mixing thoroughly. Antibiotics were used at the following concentrations: 10 μg/mL chloramphenicol (Cam), 10 μg/mL tetracycline (Tet), and 10 μg/mL trimethroprim (Tmp), 10-50 μg/mL erythromycin (Erm), 100 μg/mL kanamycin (Kan). These same concentrations were also used to grow *E. coli* with the exception of Kan (50 μg/mL), Erm (500 μg/mL), and ampicillin (Amp, 50 μg/mL). Cultures were grown aerobically (1:10 media-to-flask ratio, 250 rpm) or micro-aerobically (3:5 media-to-flask ratio, 125 rpm) at 37°C or 30°C (for temperature sensitive strains).

Phage propagation and transduction. Bacteriophage propagation: *S. epidermidis* carrying marker to be transduced were grown on TSA plates (with antibiotic if appropriate), resuspended in 100 μL of sterile saline or TSB to ~10^{10} CFU/mL. Bacteriophage (ΦA6C, Φ71, or Φ187) were serial diluted up to 10^{-7} in either sterile saline or TSB. 100 μL of each bacteriophage dilution and 10 μL of cell suspension were added to 5-mL snap cap polystyrene tubes. Finally, 4 mL of warm, melted soft agar (0.5% w/v in TSB) was added and tubes were inverted several times to mix, then poured onto fresh $CaCl_2$ plates, allowed to solidify, and stored in 30°C incubator upright overnight. On the following day, bacteriophage was harvested by adding 2-3 mL of sterile TSB to each confluent plate. The soft agar was broken up, collected in a 15- or 50-mL centrifuge tube, and centrifuged at 5000 RPM for 10 minutes. The phage lysate was filter sterilized with a 0.22 μm filter and stored at 4°C.

Transduction: Transduction was performed using bacteriophages ΦA6C, Φ71, or Φ187 (149, 150) following a modified method previously described (151). Recipient cells

were resuspended in a 15-mL centrifuge tube containing 1.5 mL of TSB+ 5 mM $CaCl_2$ and 500 µL of high titer bacteriophage (>10^8 PFU/mL). This was incubated, with shaking, for 20 minutes at 37°C (30°C for temperature sensitive plasmids), then 1 mL of cold (4°C) 0.02 M sodium citrate was immediately added and centrifuged at 5000 RPM for 10 minutes. The supernatant was discarded, the pellet resuspended in 0.02 M sodium citrate, plated on TSA + 500 mg/L sodium citrate + appropriate selecting antibiotic and incubated at 37°C (or 30°C).

SOE PCR. Splicing by overlap extension (SOE) PCR was used to clone a promoter to a different gene without the addition of enzyme restriction sites. Specifically, in this study, P*sarA* was cloned to *icaR* and *tcaR* (to generate pNF332 and pNF333) and *lacZ* was cloned to P*ica* (pNF291). The reverse primer amplifying the promoter carried 15-25 bp of the gene, allowing for overlap and annealing of this PCR product to the PCR products of the genes. Likewise, the forward primer amplifying the genes carried 15-25 bp of the 3' end of the promoter. The promoter and genes were amplified separately by PCR using Pfurther Long-Range DNA Polymerase (Monserate Biotechnology Group) then the two products were diluted, added 1:1 to a new PCR reaction (as the template) and amplified again using the forward promoter primer and the reverse primer for the genes. The joined products were used to generate allelic exchange plasmids as described below.

Construction of *tcaR* allelic replacement plasmid. All PCR reactions were performed with Pfurther Long-Range DNA Polymerase (Monserate Biotechnology Group; San Diego, CA). Primers 2038+ 2039 (BamHI, XbaI) and 2015+ 2016 (SalI, PstI) (Table 2.2) were used to amplify the 5' region and 3' region, respectively, of *tcaR* using *S. epidermidis* 1457 as the template DNA (GenBank accession number CP020463.1). These sequences were inserted into the pUC19 multiple cloning site using the corresponding restriction enzyme sites. The *dhfr* cassette (conferring for trimethroprim resistance) was amplified with primers 2234+ 2235 and inserted between the 5' and 3' *tcaR* sequences using SalI and XbaI. This construct

was then digested with PstI and ligated into pROJ6448 to generate pNF263. Cloning was performed in *E. coli* DH5α and the complete pNF263 plasmid was electroporated into electrocompetent *S. aureus* RN4220 (152, 153). Plasmid DNA was then isolated from RN4220 and electroporated into electrocompetent *S. epidermidis* 1457 and transduced into CSF41498 via bacteriophage ΦA6C.

Construction of *icaR* and *tcaR* complementation plasmids. All PCR reactions were performed with Pfurther Long-Range DNA Polymerase (Monserate Biotechnology Group). Primers 3090 (KpnI) and 3091 (*icaR)* or 3092 (*tcaR*) were used to amplify the *sarA* promoter (Table 2.2). The *icaR* and *tcaR* open reading frames were amplified with primers 3093+ 2697 (BamHI) and 3094+ 3095 (BamHI) (respectively). Because these genes were driven by the constitutive *sarA* promoter (instead of their native promoter), SOE PCR was performed to ensure the *sarA* promoter could be cloned to the gene without introduction of restriction enzyme recognition sites. The SOE PCR generated products were inserted into pCL10 using KpnI and BamHI. The 5' and 3' regions of the lipase gene were amplified with primers 3096+ 3097 (SalI, XbaI) and 3098+ 3099 (KpnI, SacI), respectively. A kanamycin resistance cassette was amplified with primers 3088 (BamHI)+ 3089 (XbaI) and inserted between the 5' and 3' lipase sequences to generate pNF332 (*icaR*) and pNF333 (*tcaR*). These plasmids were constructed in *E. coli* DH5α, electroporated into electrocompetent PS187 Δ*hsdR* Δ*sauUSI*, then transduced into *S. epidermidis* 1457 using bacteriophage Φ187.

Construction of *gdpP* allelic exchange plasmid. All PCR reactions were performed with Pfurther Long-Range DNA Polymerase (Monserate Biotechnology Group). The 5' and 3' regions of *gdpP* were amplified with primers 3227 (SacI)+ 3228 (KpnI) and 3229 (KpnI)+ 3230 (SalI), respectively. A kanamycin resistance cassette was amplified with primers 3088 (BamHI)+ 3089 (XbaI). These PCR products were inserted into pCL10 using the indicated

restriction enzyme sites in *E. coli* DH5α to generate pNF353 which was subsequently electroporated into *S. aureus* PS187 and transduced into 1457 using Φ187.

Allelic exchange. *S. epidermidis* strains carrying the cloning vector was inoculated into culture tubes containing TSB+ antibiotic, allowed to grow at 30°C, shaking, until approximately mid-exponential phase. This culture was then inoculated 1:1000 into a fresh culture tube containing TSB only and grown at 45°C overnight. Cultures were diluted 1:1000 in fresh TSB every day until single recombinants were identified as follows. Starting on the third day, cultures were serial diluted and plated on TSA+ antibiotic and grown at 45°C. These plates were then patched onto TSA+ antibiotic. PCR was used to identify single recombinants (one primer should be located outside recombination region and one primer should be within antibiotic marker). Single recombinants were inoculated into fresh culture tubes and grown as described above to generate double recombinants. To identify double recombinants, colonies were patched onto TSA+ mutant antibiotic marker (or just TSA if markerless mutant) and TSA+ vector antibiotic marker. Double recombinants were confirmed by PCR using primers located outside recombination region. When possible, mutations were backcrossed into a clean background using Φ71 or ΦA6C and confirmed by pulsed-field gel electrophoresis.

Alternative method: *S. epidermidis* carrying cloning plasmid was streaked onto TSA+ antibiotic and grown at 45°C. When grown, a few colonies (big ones if there is a size difference) were selected and streaked onto TSA+ antibiotic and grown at 45°C. This was repeated twice more before colonies were patched onto TSA+ antibiotic and grown at 45°C. Single recombinants were patched and screened using PCR (as described above). Single recombinants were inoculated into culture tubes containing TSB and grown at 30°C, shaking, and diluted 1:1000 every day. Starting on the fifth day, cultures were plated onto TSA and

grown at 30°C. Individual colonies were patched onto TSA and double recombinants are identified as described above.

Generation of P*ica*::GFP reporters. Primers 1803 and 1804 were used to amplify the *ica* promoter using 1457 genomic DNA as template. The PCR product was cloned into the BamHI and NheI sites of pIHW4 (carrying a gene encoding for superfolder GFP) in *E. coli.* to generate pNF206. The constructed reporter plasmid was electroporated into RN4220 and subsequently electroporated into 1457. Finally, pNF206 was transduced from 1457 pNF206 into 1457 Δ*icaR,* 1457 Δ*tcaR,* and 1457 Δ*icaR* Δ*tcaR* using Φ71.

Generation of IcaR and TcaR overexpression strains. Primers 2692 (NdeI)+ 2357 (BamHI) and 2358 (NdeI)+ 2359 (BamHI) were used to amplify the open reading frames of *icaR* and *tcaR,* respectively, using 1457 genomic DNA as template with Pfurther Long-Range DNA Polymerase (Monserate Biotechnology Group). These PCR products were inserted into the protein expression vector pET15b, using the indicated restriction enzyme sites, in *E. coli* BL21/DE3 to generate pNF290 (IcaR) and pNF292 (TcaR). pNF292 was transformed into chemically competent *E. coli* Arctic Express for overexpression experiments.

Expression and purification of recombinant proteins. IcaR (BL21/DE3 pNF290) was induced using Auto-induction media (adapted from (154)) for 18 hours at 37°C aerobically. To induce TcaR, Arctic Express pNF352 was grown in LB+ ampicillin aerobically at 37°C to OD_{600}=0.6 then induced with 1 mM IPTG for 3 hours. Induced cultures were then pelleted at 4°C and resuspended in equilibrium buffer (1:20) containing protease inhibitors (4 mM PMSF, 1 mM NEM, 25 mM EACA). Cells were passaged through an EmulsiFlex C3 (Avestin; Ontario, Canada) three times to lyse cells. Samples were then centrifuged at 4°C and supernatants incubated with 1 mL of HisPur cobalt resin (Pierce Biotechnology; Rockford, IL) overnight on an end-over-end mixer at 4°C. Resin was then washed and eluted following manufacturer instructions. Purified proteins were concentrated at 20°C using a Vivaspin

10,000 MWCO column (Sartorius AG; Göttingen, Germany) and stored in phosphate buffered saline (PBS) with 30% glycerol at -20°C.

Pulsed-field gel electrophoresis. Strains of interest, grown on plates or in liquid culture, were resuspended in PIV buffer to OD_{600}≈1.0. A mix of 10 µL of 1 mg/mL Lysostaphin, 200 µL of cell resuspension, and 200 µL hot, melted 1.5% agarose (in 1x TE) was prepared and quickly pipetted into plug molds. Once the plugs hardened, they were removed from the mold and placed into a 15-mL conical tube containing EC buffer and incubated at 37°C for 3-6 hours. The EC buffer was then removed and the plugs were washed with 5 mL of DI water at 54°C for 15-30 minutes twice, then washed three times in the same manner with 1x TE buffer. Plugs were stored in 1x TE buffer at 4°C.

A master mix of digest reaction (1x buffer, 1 uL of *SmaI* (Thermo Fisher; Waltham, MA), and water) was prepared. Each plug was cut to the appropriate size and added to a microcentrifuge tube containing 150 µL of digest reaction and incubated at room temperature for >3 hours. After digestion, plugs were set in a 1% agarose gel and electrophoresed in 0.5X TBE at 6 V/cm for 18 hours, at 18°C (5.0 sec initial switch time, 40 sec final switch time) using the CHEF-DR III System (Bio-Rad Laboratories; Hercules, CA). Gels were stained with ethidium bromide and visualized by UV exposure.

RNA isolation. Overnight cultures grown in TSB were diluted into flasks containing TSB to an OD_{600}= 0.05 and grown micro-aerobically. Cells were collected at the appropriate time points, pelleted at 4°C (5000 RPM), and resuspended in 900 uL of RLT buffer (containing 10% β-mercaptoethanol) (Qiagen). Cells were disrupted using a Bead Ruptor 24 (speed=6.0, 25 sec x2) (Omni International; Kennesaw, GA) and pelleted at 13,000 RPM for 10 minutes at 4°C. The supernatant was added to 500 µL of ethanol and RNA was isolated using the RNEasy Mini kit following manufacturer's protocol (Qiagen; Hilden, Germany). Purified RNA was

eluted in 40 µL of RNase-free water, quantified using a NanoDrop 2000 Spectrophotometer, and stored at -80°C.

Northern blot. RNA gel was prepared with 1% agarose in 1x AccuGENE MOPS buffer (Lonza; Rockland, ME) and 1% formaldehyde. RNA (3-5 µg) was added to 1x RNA loading buffer and heated to 75°C for 15 minutes prior to loading onto gel. Voltage is applied at 70 volts for 10 minutes then 50 volts for 7 hours in 1x AccuGENE MOPS buffer.

RNA was transferred to positively-charged nylon membrane (Roche; Basel, Switzerland) with 20X SSC buffer overnight. RNA was crosslinked to the membrane using a Stratalinker UV Crosslinker (Stratagene; La Jolla, CA) set to auto-crosslink and prehybridized in DIG Easy Hyb Buffer (Roche) for 2 hours at 50°C.

DNA probes were Digoxigenin (DIG) labeled by PCR with DIG DNA Labeling Mix (Roche), boiled for 10 minutes to denature, added to DIG Easy Hyb Buffer, and incubated with the blot overnight at 50°C. After hybridization, blots were washed twice in 2X SSC/0.1% SDS and twice more with 0.1X SSC/0.1% SDS heated to 55°C. After washing blot with 1x Washing Buffer (DIG Wash and Block Buffer Set, Roche) for 2 minutes at room temperature, the blot was blocked in 1X Blocking Solution for 30 minutes at room temperature. Anti-Digoxigenin-AP Fab (Roche) was diluted 1:10,000 in 1X Blocking Solution and incubated with the blot for 1 hour at room temperature. Blot was washed with 1X Washing Buffer for 15 minutes twice at room temperature, incubated with ECF chemiluminescent substrate (GE Healthcare Life Sciences; Piscataway, NJ) for 20-30 minutes and visualized on a Typhoon FLA 7000 (GE Healthcare Life Sciences).

Quantitative real-time PCR. 500 ng of total RNA was converted to cDNA with the QuanTect Reverse Transcription Kit (Qiagen) and diluted 1:50 in RNase-free water. Primers were diluted to a concentration of 5 µM each and combined. 10 µL of diluted cDNA was combined with 2 µl of combined primers, 8 µL RNase-free water, and 20 µL LightCycler 480

Sybr green I master mix (Roche). The reaction was divided into two wells (19 µL each) of a white 96-well conical plate. Real-time PCR was performed on a Roche LightCycler 480 II. Quantified expression values were normalized to *gyrB* expression levels and reported as fold-change compared to wild-type.

PIA immunoblot assay. Bacterial cultures were collected to an adjusted OD_{600}=5, pelleted by centrifugation (5000 RPM, 5 minutes), resuspended in 500 µL of TE buffer and boiled for five minutes. Cells were again pelleted by centrifugation and 190 µL of the supernatant was moved to a new tube containing 10 µL of proteinase K. After incubation at 37°C for one hour, proteinase K was inactivated by boiling for an additional 10 minutes and isolated PIA samples were stored at -20°C.

PIA preparations were diluted 1:10 and 1:100 in tris buffered saline (TBS). 100 µL of each dilution was applied to a 0.45 µm nitrocellulose membrane (Bio-Rad Laboratories) using a Bio-Dot Microfiltration Apparatus (Bio-Rad Laboratories). Membrane can be air-dried and stored at 4°C.

Membrane was hydrated in TBS and blocked with 5% milk (powdered, w/v) in TBS + 0.01% tween-20 (T-TBS) for 2-4 hours at room temperature, then incubated with anti-PIA primary antibody (gift from Jim O'Gara) (1:20,000 in 1% milk in T-TBS) overnight at 4°C. After washing three times with T-TBS, the blot was incubated with alkaline phosphatase-conjugated goat anti-rabbit secondary antibody (Jackson Immunoresearch; West Grove, PA) (1:25,000 in T-TBS) for one hour, at room temperature, before detection with ECF chemiluminescent substrate (GE Healthcare Life Sciences) and visualization on a Typhoon FLA 7000 (GE Healthcare Life Sciences).

Static biofilm assay. A 96-well flat bottom Delta Surface plate (Corning) was filled with 198 µL of sterile TSB and inoculated with 2 µL of cells (from an overnight culture or resuspended from a plate to ~OD_{600}=1.0 in TSB or PBS). Cultures were grown statically at

37°C for ~24 hours. Media were removed and wells were washed with PBS three times. Plates were dried (inverted) at 45°C for 2 hours and stained with 150 µL of crystal violet stain for 15 minutes at room temperature. Stain was removed and plate was washed under running water until water runs colorless. Crystal violet stain was solubilized with 95% ethanol for more consistent quantification on a plate reader (OD_{595}).

BioFlux biofilm assay. *S. epidermidis* strains were grown overnight micro-aerobically and diluted to OD_{600}=0.8 in 50% TSB. Channels of a BioFlux1000 48-well plate were primed by adding 200 µL 50% TSB to the output wells and reversing flow for 5 minutes at 5.0 dynes/cm^2 using a BioFlux1000 microfluidic system (Fluxion Biosciences, Inc., San Francisco, CA). The excess TSB was removed and the channels were seeded by adding the diluted cultures to the output wells and pumping backwards through the channels at 2.0 dynes/cm^2 for 2 seconds. The plates were incubated at 37°C for 1 hour to allow cells to adhere to the channel surface. The output wells were then emptied and 1.3 mL of fresh 50% TSB was added to the input wells. The assay was initiated by pumping media at a rate of 0.6 dynes/cm^2 at 37°C for 18 hours. Bright-field and epifluorescence images (using a FITC filter) were acquired every 5 minutes.

Hemocyanin conjugation. Hemocyanin (Hcy; Sigma) was dissolved in $NaHCO_3$ to a concentration of 5 mg/mL and 1 mg was combined with 1 mg of IcaR antigen (molar ratio should be 120:1 IcaR:Hcy). Glutaraldehyde (Grade II; Sigma) was prepared in $NaHCO_3$ to a concentration of 25 mM and 100 µL was added to Hcy+Icar mix and incubated overnight at room temperature.

Western blot analysis. Concentration of protein samples were determined using a NanoDrop 2000 Spectrophotometer (Thermo Scientific) or with Bradford assay. Samples were adjusted for equal protein amount (100 ug total protein for cell lysates, 50 ng for purified proteins) and mixed with 4x SDS loading buffer, denatured at 95°C for 10 minutes,

then loaded on a 14% SDS-PAGE gel. Current was applied at 50 volts for 30 minutes and 150 volts until dye front reaches bottom of gel. Proteins were transferred onto a PVDF membrane in cold 1x transfer buffer, at 100 volts for 1 hour. Membrane was then washed briefly with T-TBS, blocked with 5% milk in T-TBS for 2-4 hours at room temperature, then incubated with primary antibody (anti-IcaR serum) (1:1000 in 1% milk in TBS-T) at 4°C overnight. After washing membrane T-TBS three times, the blot was incubated with HRP-conjugated goat anti-rabbit secondary antibody (Jackson Immunoresearch) (1:25,000 in TBS-T) for 1 hour at room temperature. Finally, the membrane was washed three times with T-TBS. Detection was performed with SuperSignal West Pico chemiluminescent substrate (Thermo Scientific) and Azure C600 imaging system (Azure Biosystems; Dublin, CA) or by autoradiography film.

Electrophoretic mobility shift assay (EMSA). Primers 2850, 2851 were used to amplify the *ica* promoter carrying a fluorescein tag. Increasing concentrations (100-1000 pmol) of recombinant IcaR and TcaR were incubated with labeled DNA in binding buffer (20 mM Tris-HCl pH 8.0, 150 mM KCl, 0.1 mM $MgCl_2$, 0.05 mM EDTA, 12.5% glycerol, 10 mM DTT, 1 mg/mL BSA) for 30 minutes at room temperature. 10 µL of 10 mg/mL salmon sperm DNA was added as noncompetitive DNA. 15.8 µM of unlabeled DNA (amplified with primers 2865, 2851) was added as competitive DNA. After incubation, loading buffer was added to each reaction and loaded onto a 6% polyacrylamide gel (0.5X TBE, 0.2% glycerol, 6% Bis-acrylamide, TEMED, APS). Samples were electrophoresed in 0.5%X TBE and visualized on a Typhoon FLA 7000 (GE Healthcare).

Generation of P^{32} labeled DNA. Primer 2855 was labeled with P^{32} by incubating it with 10x kinase buffer, T4 polynucleotide kinase, and ^{32}P-ATP for 30 minutes at 37°C. The primer was then precipitated with ammonium acetate, glycogen and ice cold ethanol, incubated on dry ice for 10 minutes, pelleted by centrifugation, and washed with cold 70%

ethanol. A SpeedVac concentrator (Thermo Scientific) attached to a vacuum pump was used to dry the pelleted, labeled primer.

The *icaR-icaA* intergenic region was amplified using labeled primer 2855 and unlabeled primer 2965 and HiFi Platinum Taq polymerase (Invitrogen; Carlsbad, CA) with 1457 genomic DNA as the template. Labeled PCR product was cleaned using the Wizard SV Gel and PCR Clean-up System (Promega; Madison, WI).

DNase I footprinting assay. Labeled DNA was incubated with protein in binding buffer (20 mM Tris-HCl pH 8.0, 150 mM KCl, 0.1 mM $MgCl_2$, 0.05 mM EDTA, 12.5% glycerol, 10 mM DTT, 1 mg/mL BSA), to a final volume of 20 µL, for fifteen minutes at room temperature. 20 µL of 5 mM $CaCl_2$/ 10 mM $MgCl_2$ was added to each reaction followed by 10 µL of diluted DNase I. 100 µL STOP buffer (0.125% SDS, 12.5 mM EDTA, 3 mg/mL glycogen) was added exactly one minute after the addition of DNase I and the reaction was placed on ice. 100 µL of phenol:choloroform:isoamyl alcohol (25:24:1) was added, the reaction was mixed by flicking, and centrifuged to separate the layers. The aqueous layer was moved to a new tube containing 1 mL of ice cold ethanol and stored at -20°C overnight (or on dry ice for 15 minutes). The DNA was pelleted by centrifugation for 20 minutes, the ethanol was removed, and the pellet was washed with 70% ethanol. A SpeedVac concentrator (Fisher Scientific) was used to dry the pellet. The pellet was then resuspended in 7 µL of loading buffer (7 M urea, 0.1X TBE, 0.05% Bromophenol blue, 0.05% Xylene cyanol FF), heated at 95°C for two minutes in a thermal cycler, and loaded onto a 6% denaturing polyacrylamide gel (42% urea, 1X TBE, 6% polyacrylamide, TEMED, APS). The gel was electrophoresed on a pre-warmed (50°C) Sequi-Gen GT Nucleic Acid Electrophoresis Cell (Bio-Rad) apparatus at 50 watts in 0.5X TBE until the dye front migrates ¾ of the way through the gel, maintaining buffer temperature at 50-55°C. The gel was then transferred onto a large piece of Whatman

paper (GE Healthcare), covered in plastic wrap, and dried on a gel dryer attached to a vacuum pump. Finally, the dried gel was developed using autoradiography film.

Flow cell biofilms. Stovall flow cells (IBI Scientific; Dubuque, IA) were filled with sterile TSB and inoculated with 100 µL of overnight culture. Cells were allowed to adhere to the surface for 1 hour at 37°C then sterile TSB was continuously pumped through the channel at a rate of 500 µL/minute for 24 hours at 37°C.

Isolation of biofilm mutants. 25 cm^2 polystyrene tissue culture flasks (Corning Life Sciences; Durham, NC) were filled with 5 mL of sterile TSB and inoculated with a single colony of *S. epidermidis*. The flask was incubated at 37°C statically and fresh media was replaced every day. On day 5, the flasks were washed with sterile saline and cells were removed from the flask using a cell scraper (Biologix Corp; Shandong, China). The biofilms were dispersed using a Sonic Dismembrator (Fisher Scientific) on setting 1, serial diluted and plated on Congo Red Agar.

Congo red agar (CRA) assay. PIA production was screened on Congo red agar as previously described (155). Agar contained 30 g TSB (Becton Dickinson Difco), 15 g granulated agar (Becton Dickinson Difco), 36 g sucrose (Sigma), and 0.8 g Congo red (Sigma) per liter of distilled water. Strains were streaked or spread plated on agar, allowed to grow at 37°C for ~24 hours.

Sequencing of biofilm mutants. Genomic DNA was isolated from overnight cultures of the mutants using the Wizard Genomic DNA Purification Kit (Promega). Sequencing was performed as previously described (156). RS II (Pacific Biosciences, USA) single-molecule real-time sequencing (SMRT) produced reads that were assembled using HGAP2 in the SMRT Analysis Portal. MiSeq (Illumina, Inc., USA) short-read sequencing produced reads with an average length of 350 bp and insert size of 500 bp which were mapped to the trimmed SMRT

sequences using Geneious software (Biomatters, New Zealand). Genes were predicted using the NCBI Prokaryotic Genome Annotation Pipeline version 4.5.

β-galactosidase assay. Bacterial cultures were pelleted by centrifugation and resuspended in 1.2 mL of Z-buffer (60 mM Na_2HPO_4, 40 mM NaH_2PO_4, 10 mM KCl, 1 mM $MgSO_4$, 50 mM β-mercaptoethanol, pH 7.0) in a screw-cap tube containing 1 mM glass beads. Cells were lysed by disruption using a Bead Ruptor 24 (speed=6.0, 25 sec x2) (Omni International). The contents were then pelleted by centrifugation and 700 μL of the supernatant was transferred to a microcentrifuge tube. The reaction was initiated by addition of 140 μL of 4 mg/mL ONPG and incubated at 37°C. Once the sample turned yellow, the reaction was stopped with 200 μL of 1 M sodium carbonate and the reaction time was noted. The stopped reaction was centrifuged for 30 seconds and OD_{420} was measured. β-galactosidase activity was adjusted for protein concentration as determined by Bradford reaction using the Protein Assay Dye Solution (Bio-Rad).

Table 2.1 Bacterial strains, plasmids, and bacteriophages used in this study

Strain	Description	Source
Escherichia coli DH5α	Cloning host	Invitrogen
S. aureus RN4220	Restriction deficient, modification positive	[166][44]
S. aureus PS187	Cloning host, Φ187 propagation strain	[150]
E. coli BL-21 (DE3)	Protein over-expression strain	Invitrogen
E. coli Arctic Express	Protein over-expression strain, adapted for growth at low temperatures	Agilent Technologies
S. epidermidis 1457	High PIA and biofilm producing strain	[161]
S. epidermidis CSF41498	*icaADBC* positive, biofilm producing strain	[87]
S. epidermidis 1457 *icaA::dhfR*	1457 *icaA* deletion mutant, Tmp^R	[106]
S. epidermidis 1457 *icaR::tetM*	1457 *icaR* deletion mutant, Tet^R	[106]
S. epidermidis CSF41498 *icaR::erm*	CSF41498 *icaR* mutant, Erm^R	[87]
S. epidermidis 1457 *tcaR::dhfR*	1457 *tcaR* deletion mutant, Tmp^R	This study
S. epidermidis CSF41498 *tcaR::dhfR*	CSF41498 *tcaR* deletion mutant, Tmp^R	This study
S. epidermidis 4804	*icaADBC* positive clinical isolate	[90]
S. epidermidis 5595	*icaADBC* positive clinical isolate	[90]
S. epidermidis 7613	*icaADBC* positive clinical isolate	[90]
S. epidermidis 8595	*icaADBC* positive clinical isolate	[90]
S. epidermidis 8889	*icaADBC* positive clinical isolate	[90]
S. epidermidis 9958	*icaADBC* positive clinical isolate	[90]
S. epidermidis 5387	*icaADBC* positive clinical isolate	[90]
S. epidermidis 1457 *icaR::tetM geh::icaR::kan*	1457 *icaR* mutant carrying *icaR cis* complementation, driven by constitutive *sarA* promoter, Tet^R, Kan^R	This study
S. epidermidis 1457 *tcaR::dhfR geh::tcaR::kan*	1457 *tcaR* mutant carrying *tcaR cis* complementation, driven by constitutive *sarA* promoter, Tmp^R, Kan^R	This study
S. epidermidis 1457 *icaR::tetM tcaR::dhfR geh::tcaR::kan*	1457 *icaR tcaR* double mutant carrying *tcaR cis* complementation, driven by constitutive *sarA* promoter, Tmp^R, Kan^R	This study
S. epidermidis CSF41498 *icaR::erm geh::icaR::kan*	CSF41498 *icaR* mutant carrying *icaR cis* complementation, driven by constitutive *sarA* promoter, Kan^R	This study

S. epidermidis CSF41498 *tcaR::dhfR geh::tcaR::kan*	CSF41498 *tcaR* mutant carrying *tcaR cis* complementation, driven by constitutive *sarA* promoter, Kan^R	This study
S. epidermidis CSF41498 *icaR::erm tcaR::dhfR geh::tcaR::kan*	CSF41498 *icaR tcaR* double mutant carrying *tcaR cis* complementation, driven by constitutive *sarA* promoter, Tmp^R, Kan^R	This study
S. epidermidis 7613 *icaR::tetM*	7613 *icaR* deletion mutant, Tet^R	This study
S. epidermidis 7613 *tcaR::dhfR*	7613 *tcaR* deletion mutant, Tmp^R	This study
S. epidermidis 9958 *icaR::tetM*	9958 *icaR* deletion mutant, Tet^R	This study
S. epidermidis 9958 *tcaR::dhfR*	9958 *tcaR* deletion mutant, Tmp^R	This study
S. epidermidis A9	CSF41498 enhanced PIA producing mutant	This study
S. epidermidis A9 *icaR::tetM*	A9 *icaR* deletion mutant, Tet^R	This study
S. epidermidis P4	CSF41498 enhanced PIA producing mutant	This study
S. epidermidis P4 *icaR::tetM*	P4 *icaR* deletion mutant, Tet^R	This study
S. epidermidis C9	CSF41498 enhanced PIA producing mutant	This study
S. epidermidis C9 *icaR::tetM*	C9 *icaR* deletion mutant, Tet^R	This study
S. epidermidis C9 *tcaR::dhfR*	C9 *tcaR* deletion mutant, Tmp^R	This study
S. epidermidis N2	CSF41498 enhanced PIA producing mutant	This study
S. epidermidis N2 *icaR::tetM*	N2 *icaR* deletion mutant, Tet^R	This study
S. epidermidis N2 *tcaR::dhfR*	N2 *tcaR* deletion mutant, Tmp^R	This study
S. epidermidis O7	CSF41498 enhanced PIA producing mutant	This study
S. epidermidis O7 *icaR::tetM*	O7 *icaR* deletion mutant, Tet^R	This study
S. epidermidis O7 *tcaR::dhfR*	O7 *tcaR* deletion mutant, Tmp^R	This study
S. epidermidis D9	CSF41498 enhanced PIA producing mutant	This study
S. epidermidis D9 *icaR::tetM*	D9 *icaR* deletion mutant, Tet^R	This study
S. epidermidis D9 *tcaR::dhfR*	D9 *tcaR* deletion mutant, Tmp^R	This study

S. epidermidis PV22 *icaR::tetM*	PV22 *icaR* deletion mutant, Tet^R	This study
S. epidermidis PV22 *tcaR::dhfR*	PV22 *tcaR* deletion mutant, Tmp^R	This study
S. epidermidis 22R5	1457 mutant defective in PIA synthesis	[155]
S. epidermidis 22R5 *icaR::tetM*	22R5 *icaR* deletion mutant, Tet^R	This study
S. epidermidis 22R5 *tcaR::dhfR*	22R5 *tcaR* deletion mutant, Tmp^R	This study
S. epidermidis 22R6	1457 mutant defective in PIA synthesis	[155]
S. epidermidis 22R6 *icaR::tetM*	22R6 *icaR* deletion mutant, Tet^R	This study
S. epidermidis 22R6 *tcaR::dhfR*	22R6 *tcaR* deletion mutant, Tmp^R	This study
S. epidermidis 1457 *icaADBC*::P*ica::lacZ*	1457 *icaADBC* deletion mutant replaced with *lacZ* driven by *ica* promoter, Tmp^R	This study
S. epidermidis CSF41498 *icaADBC*::P*ica::lacZ*	CSF41498 *icaADBC* deletion mutant replaced with *lacZ* driven by *ica* promoter, Tmp^R	This study
S. epidermidis 1457 Δ*gdpP*	1457 *gdpP* in-frame deletion mutant	This study
S. epidermidis CSF41498 Δ*gdpP*	CSF41498 *gdpP* in-frame deletion mutant	This study

Plasmid	Description	Source
pUC19	Gram-negative origin of replication, Amp^r	Invitrogen
pROJ6448	pE194 containing pC221 nick site functioning in conjugative mobilization, temp sensitive gram-positive origin of replication, Erm^r	[167]
pCL10	Temperature-sensitive shuttle vector	[168]
pET15-b	Protein over-expression vector, N-terminal His-tag	Invitrogen
pNF206	P*ica*::GFP reporter, Erm^R, Amp^R	This study
pNF263	*tcaR* mutagenesis plasmid	this study
pNF290	IcaR protein expression vector, pET-15b backbone, Amp^R	This study
pNF291	*icaADBC* allelic exchange plasmid, carries P*ica::lacZ*, pCL10 backbone, Cam^R, Amp^R, Tmp^R	This study
pNF292	TcaR protein expression vector, pET-15b backbone, Amp^R	This study
pNF332	lipase allelic exchange plasmid, for generation of constitutive *icaR* complement strain, pCL10 backbone, Cam^R, Amp^R, Kan^R	this study
pNF333	lipase allelic exchange plasmid, for generation of constitutive t*caR* complement strain, pCL10 backbone, Cam^R, Amp^R, Kan^R	this study

pNF353	Allelic exchange plasmid, for generation of in-frame *gdpP* deletion mutant, pCL10 backbone, Cam^R, Amp^R	this study
pBursa	Encodes *bursa aurealis* transposon, Cam^R, Erm^R	[169]
pFA545	Encodes *bursa aurealis* transposase, Tet^R	[169]

Bacteriophage	Description	Source
Φ71	*S. epidermidis* transducing phage	[170]
ΦA6C	*S. epidermidis* transducing phage	[149]
Φ187	Staphylococcus transducing phage	[150]

Abbreviations: Amp, ampicillin; Tet, tetracycline; Erm, erythromycin; Tmp, trimethroprim; Cam, chloramphenicol; Kan, kanamycin

Table 2.2. Primers used in this study

Primer	Sequence	Product, direction, restriction site	Purpose
2038	GGGCCCGGATCCCGTGTATTCGTGGATTGATTC	5' *tcaR*, forward, BamHI	Generation of *tcaR* mutagenesis allelic exchange plasmid, pNF263
2039	GGGCCCTCTAGAGCTCAGCTGATATGCCATACTC	5' *tcaR*, reverse, XbaI	
2015	GGGCCCGTCGACGCGATTATGAGCCATATTGC	3' *tcaR*, forward, SalI	
2016	GGGCCCCTGCAGGCTTCAGCAATGACAGTTTTC	3' *tcaR*, reverse, PstI	
2234	GGCCGTCGACCGATTGTCAGGCTTAATGG	Trimethroprim, forward, SalI	
2235	GGCCTCTAGAGCAACTTAGGGAATGTTTATGG	Trimethroprim, reverse, XbaI	
2273	GCCCATTGAATGTACCGTTT	*tcaR* confirmation, forward	
2274	CACACAACATCTGACTTGAA	*tcaR* confirmation, reverse	
1803	CGCGGATCCCTTTATCCAAAGCGATGTGCGTAGG	*ica* promoter, forward, BamHI	Generation of P*ica*::GFP reporter, pNF206
1804	CGCGCTAGCCGTTAGTTAGGTTGTAAAGCATATGC	*ica* promoter, reverse, NheI	
2692	GGAATTCATATGTTGAAAGATAAGATTATTGATAACGC	*icaR*, forward, NdeI	Generation of IcaR over-expression vector, pNF290
2357	CCCGGATCCTTATTTTTTTAAAAATACATTTAACAGTG	*icaR*, reverse, BamHI	
2358	GGAATTCCATATGATGGTAAGAAGAATAGAAGATCACATC	*tcaR*, forward, NdeI	Generation of TcaR over-expression vector, pNF292
2359	CCCGGATCCTCAAAGTTTAGAAGTATAAGATTGTAT	*tcaR*, reverse, BamHI	

3090	GCCGCGGGTACCTGTTTACTTCTTAATTTTATTT	P*sarA*, forward, KpnI	
3091	*AATCTTATCTTTCAT*TAATGAAACCTCCCTATTTA	P*sarA* , reverse, SOE	
3092	*TATTCTTCTTACCAT*TAATGAAACCTCCCTATTTA	P*sarA* , reverse, SOE *tcaR*	
3093	*TGATATAAATAGGGAGGTTTCATTA*ATGAAAGATAAGATTATTGAT	*icaR* reverse, SOE	
3094	*TGATATAAATAGGGAGGTTTCATTA*ATGGTAAGAAGAATAGAAGATCA	*tcaR* forward, SOE	For generation of *icaR*, *tcaR* complementation *geh* allelic exchange plasmid, pNF332 and pNF333
3095	GCCGGCGGATCCGGCATTGACTCATTTTATCACCT	*tcaR*, reverse, BamHI	
2697	GGGCCCGGATCCCTCGAATTTGTTACATACTAG	*icaR*, reverse, BamHI	
3096	GCCGCGTCTAGAGGATTGGAAGCCTGGTCAAA	3' lipase, forward, XbaI	
3097	GCCGCGGTCGACAACACCCTATCCGCTCACAA	3' lipase, reverse, SalI	
3098	GCCGCGGACGTCCGAGATGGTGCATATGTGTGT	5' lipase, forward, SacI	
3099	GCCGCGGGTACCTGTTGGGGTTGTACTAGGCT	5' lipase, reverse, KpnI	
3304	GACTGCTATGATGTGACGCA	Lipase, forward	Confirmation primers for allelic exchange
3305	ATCGAACCACCCACTGCTAA	Lipase, reverse	

Enzyme restriction sites are underlined, complementary overhangs for SOE PCR are italicized

2946	CGCGGCGAGCTCGGAGGCTCTAAAATACCAAGTCT	*ica* promoter, forward, SacI	Generation of P*ica::lacZ* reporter, pNF291
2593	*CTGTAATCATTGTCATTCTAGACAT*TTTTTCACCTACCTTTCGTTAGTTAGG	*ica* promoter, reverse, SOE	
2594	*CCTAACTAACGAAAGGTAGGTGAAAAA*ATGTCTAGAATGACAATGATTACAG	*lacZ*, forward, SOE	
2947	CGCGGCCCCGGGTTATTTTTGACACCAAACTAATTG	*lacZ*, reverse, PstI	
2950	CCGCGCGGATCCTTTTCGGCACCCCTAGTTTT	*icaC*, forward, BamHI	
2951	CCGCGCGTCGACTCTTAACATCATTCCGACGCC	*icaC*, reverse, SalI	
2948	CCGCGCCCCGGGGCAACTTAGGGAATGTTTATGG	Trimethroprim cassette, XmaI	
2949	CCGCGCGGATCCCGATTGTCAGGCTTAATGG	Trimethroprim cassette, BamHI	
2902	AGGCTGGTATTGGTCAAATTGT	*icaC*, reverse	Confirmation/ sequencing primer for P*ica::lacZ* reporter integrated into *icaADBC*
2301	CTCGAAGCGGTTCGTAAAAG	*gyrB*, forward	qRT-PCR
2302	TACCACGGCCATTGTCAGTA	*gyrB*, reverse	
2710	TCAGAAATCAAACACCATCTTCAA	*icaR*, forward	qRT-PCR
2711	AGGAGGCTCTAAAATACCAAGTCT	*icaR*, reverse	
2600	TTTTCGGCACCCCTAGTTTT	*icaR*, reverse	Used with 2692 to generate northern blot probe
2850	[FLC]TTCTAAAATCTCCCCCTTAT	*ica* promoter, forward, fluorescein labelled	To amplify fluorescein-labeled and unlabeled *ica* promoter DNA for EMSA
2865	TTCTAAAATCTCCCCCTTAT	*ica* promoter, forward	
2851	TTTTTCACCTACCTTTCGTT	*ica* promoter, reverse	

2855	TACCATCGTACCCCTTTTCG	*icaR*, forward	To amplify *ica* promoter DNA for DNase I footprinting assays
2965	ACAATGATCGATTAAAGGGTTT	*icaA*, reverse	
3227	GCGGCCGAGCTCTAAAATTCCGACGGCAGCTG	5' *gdpP*, forward, SacI	For generation of *gdpP* allelic exchange plasmid
3228	GCGGCCGGTACCTGCCGAGATGTGACCACTTA	5' *gdpP*, reverse, KpnI	
3229	GCGGCCGGTACCTGACAAATGCTGCGACACAA	3' *gdpP*, forward, KpnI	
3230	GCGGCCGTCGACACGACTCAGGAAGCAAGACT	3' *gdpP*, reverse, SalI	
3231	ATGGGAGTGGCGTATGTGTT	*gdpP* confirmation, forward	
3232	AGCTTACCTACCGCAATCGT	*gdpP* confirmation, reverse	
3088	GCCGCGGGATCCAAGCTAGGGGTTTCAAAATCGG	kanamycin cassette, forward	
3089	GCCGCGTCTAGAAAAGTACGTATATAGCTTCCA	kanamycin cassette, reverse	
3090	GCCGCGGGTACCTGTTTACTTCTTAATTTTATTT	P*sarA*, forward, KpnI	For generation of *icaR, tcaR* complementation *geh* allelic exchange plasmid, pNF332 and pNF333
3091	*AATCTTATCTTTCAT*TAATGAAACCTCCCTATTTA	P*sarA* , reverse, SOE	
3092	*TATTCTTCTTACCAT*TAATGAAACCTCCCTATTTA	P*sarA* , reverse, SOE *tcaR*	
3093	*TGATATAAATAGGGAGGTTTCATTA*ATGAAAGATAAGATTATTGAT	*icaR* reverse, SOE	
3094	*TGATATAAATAGGGAGGTTTCATTA*ATGGTAAGAAGAATAGAAGATCA	*tcaR* forward, SOE	
3095	GCCGGCGGATCCGGCATTGACTCATTTTATCACCT	*tcaR*, reverse, BamHI	
2697	GGGCCCGGATCCCTCGAATTTGTTACATACTAG	*icaR*, reverse, BamHI	
3096	GCCGCGTCTAGAGGATTGGAAGCCTGGTCAAA	3' lipase, forward, XbaI	
3097	GCCGCGGTCGACAACACCCTATCCGCTCACAA	3' lipase, reverse, SalI	
3098	GCCGCGGACGTCCGAGATGGTGCATATGTGTGT	5' lipase, forward, SacI	
3099	GCCGCGGGTACCTGTTGGGGTTGTACTAGGCT	5' lipase, reverse, KpnI	
3304	GACTGCTATGATGTGACGCA	Lipase, forward	Confirmation primers for allelic exchange
3305	ATCGAACCACCCACTGCTAA	Lipase, reverse	

Enzyme restriction sites are underlined, complementary overhangs for SOE PCR are italicized

CHAPTER 3

Investigation into IcaR and TcaR regulation of *icaADBC*

Background

Expression of *icaADBC* is carefully regulated in *S. epidermidis*. This is evident by the numerous regulators identified thus far (Figure 1.2) as well as observations that the presence of the *ica* operon is not directly correlated with PIA synthesis and biofilm formation (58, 64, 90, 146-148). Therefore, our goal is to investigate why this may be and to better understand how regulation of *icaADBC* differs in different strains of *S. epidermidis.*

As previously discussed, the regulation of *icaADBC* involves many factors, including the direct repressor IcaR. Belonging to the TetR family of transcriptional regulators and originally identified in *S. aureus*, *icaR* is located upstream of *icaADBC* and is divergently transcribed (107, 112). In *S. aureus, icaR* transcription was shown to begin 73 nucleotides upstream of the *icaR* start site in the *icaR-icaA* intergenic region (106) (Figure 1.1). While regulation of *icaR* is not well understood, it has been shown to involve some environmental factors, including NaCl (σ^B dependent) and ethanol (σ^B independent).

In addition to IcaR, TcaR is also a direct repressor of *icaADBC* although this regulation is weak compared to IcaR (112, 157). TcaR was shown to regulate *icaADBC* by binding to the *icaR-icaA* intergenic region by binding to a 33-bp pseudopalindromic sequence (111). (Figure 1.1). Additional information on TcaR and its role in regulating *icaADBC* in *S. epidermidis* is limited.

Due to their role as direct repressors, we chose to further investigate the role of IcaR and TcaR with the goal of determining whether (and how) they are involved in the diverse expression of *icaADBC.* Using immunoblots and transcriptional analyses, we showed that *icaADBC* transcription and PIA synthesis is variable amongst *S. epidermidis* clinical isolates suggesting a disparity in regulation. While both IcaR and TcaR can function as regulators of *icaADBC*, IcaR seems to be the major regulator in some strains but not others. In addition to regulation of *icaADBC*, we also performed experiments to further understand the regulation

of IcaR and TcaR. Overall, our results expand on current knowledge about regulation of *icaADBC* and PIA synthesis as well as two of its repressors.

Results

***S. epidermidis* 1457 and CSF41498 differ in *icaA* transcript, PIA synthesis and biofilm formation.** Our previous results and those of others (58, 64, 90, 146-148) have shown that biofilm and PIA levels are variable amongst *icaADBC*-positive clinical isolates of *S. epidermidis*. This suggests that PIA is regulated differently in *S. epidermidis.* To further investigate differences in PIA synthesis, we chose to study strains 1457 and CSF41498, two genetically amenable strains that differ in their *in vitro* biofilm production and synthesis of PIA. As shown in Figure 3.1A, enhanced *icaA* transcript is detected in 1457 as compared to 1457 Δ*icaA* and CSF41498. In addition, 1457 produces more PIA as detected by immunoblot (Figure 1B) in addition to *in vitro* biofilm as assessed using the Christensen biofilm assay (Figure 1C).

***icaADBC* is regulated by IcaR and TcaR.** While IcaR has been well described as a direct repressor of *icaADBC* in both *S. aureus* and *S. epidermidis* (87, 88, 109, 112), the function of TcaR is less understood. Based on the observation that PIA synthesis and *icaA* transcription were variable in clinical isolates of *S. epidermidis,* we hypothesized that IcaR and/or TcaR was non-functional in strains producing excess PIA (due to de-repression of *icaADBC*). To address this hypothesis, we chose to study strains 1457, which produces excess PIA, and CSF41498, which makes very low amounts of PIA unless induced by NaCl (Figure 3.2). Notably, bioinformatic

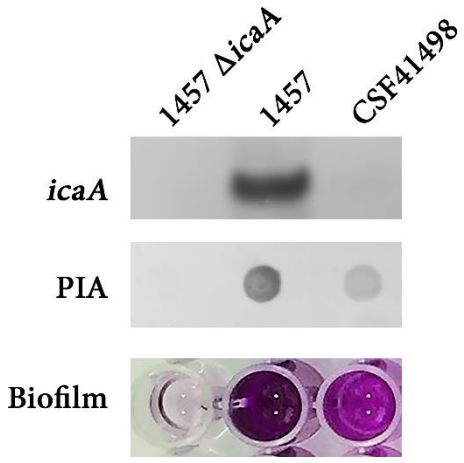

Figure 3.1. *S. epidermidis* 1457 and CSF41498 differ in *icaA* transcription. In comparison to 1457, less *icaA* transcript, PIA and biofilm were detected in CSF41498. RNA was isolated from mid-exponential phase during microaerobic growth. PIA was purified from post-exponential phase. Biofilm was stained with crystal violet after 24 hours of growth in TSB.

analysis of the 1457 and CSF41498 genomes (accession numbers CP020463.1 and CP030246) showed no sequence divergence in *icaR, tcaR, icaADBC* or the *icaR-icaA* intergenic region. *icaR*

and *tcaR* allelic replacement mutants were constructed in both 1457 and CSF41498 to assess biofilm, PIA synthesis and *icaA* transcription. As expected and previously reported, deletion of *icaR* in CSF41498 resulted in increased *icaA* transcription and enhanced biofilm and PIA synthesis (87, 88). However, inactivation of *icaR* in 1457 yielded no discernable phenotype with regards to *icaA* transcription, biofilm or PIA production (Figure 3.2). In contrast to *icaR,* deletion of *tcaR* in 1457 resulted in substantially increased *icaA* transcription, PIA synthesis, and biofilm formation indicating that TcaR functions as a repressor in 1457. Similar levels were observed in 1457 Δ*icaR* Δ*tcaR*. Conversely, *icaA* transcription, PIA synthesis, and biofilm are undetectable in CSF41498 Δ*tcaR* however, when both *icaR* and *tcaR* are knocked out, *icaA* transcript level was higher than in CSF41498 Δ*icaR*. This suggests a synergistic effect between IcaR and TcaR, and confirm previous observations made in *S. aureus* (112). Finally, complementation of *icaR* and *tcaR* resulted in complete inhibition of *icaA* transcription, suggesting that IcaR and TcaR are functional in 1457 and CSF41498. Additionally, when *icaR* was complemented into the *icaR tcaR* double mutants, *icaA* transcription was also abolished. Since *icaR* is the only functional repressor in this strain, it showed that IcaR, when expressed at high enough levels, is capable of completely repressing *icaADBC* expression. Collectively, these data suggest that IcaR is the dominant repressor in CSF41498 while TcaR appears to be dominant in 1457 (due to lack of *icaR* expression).

Alterations in *tcaR* expression affects growth. Expression of *icaADBC* and PIA synthesis is linked to the availability of glucose and the metabolic state of the cell (62, 91). For this reason, the growth of *S. epidermidis* was assessed when the regulation of *icaADBC* was altered by

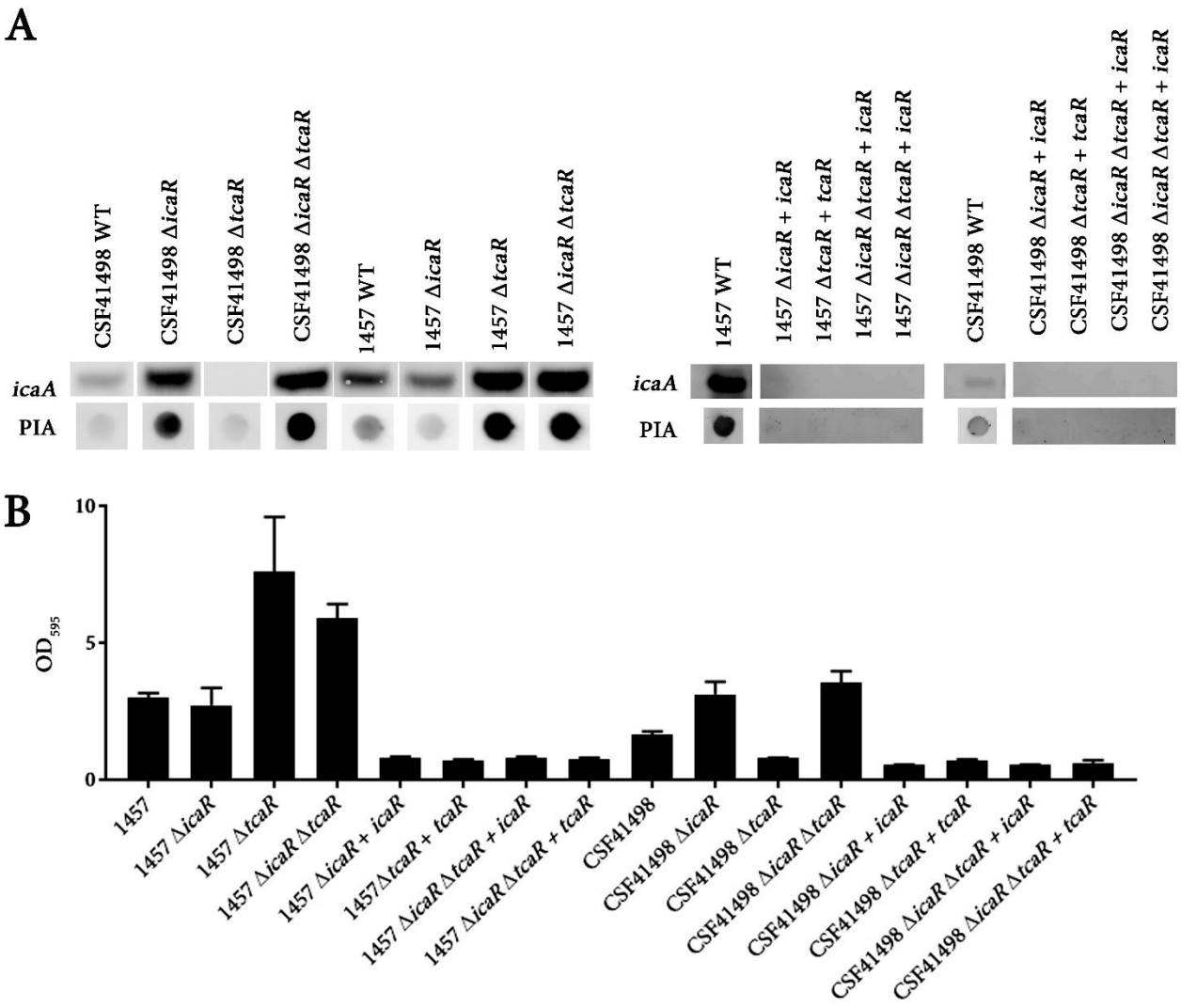

Figure 3.2. TcaR is the primary repressor in 1457 and IcaR is the major repressor in CSF41498. In 1457, inactivation of *tcaR* lead to increased *icaA* transcription, PIA synthesis, and biofilm formation while the *icaR* mutant did not have a discernable effect. In contrast, CSF41498 Δ*icaR* had increased *icaA* transcription while CSF41498 Δ*tcaR* did not. Complementation of *icaR* and *tcaR* with a constitutive promoter resulted in abolishment of *icaA* transcription and PIA synthesis. *icaR, tcaR,* and *icaR tcaR* mutants were generated in *S. epidermidis* 1457 and CSF41498 as well as constitutive *cis* complements of *icaR* and *tcaR*. *icaA* transcription was determined by northern blot and PIA synthesis was determined by immunoblot with PIA-specific antibody (A). Biofilm formation was ascertained by Christensen biofilm assay and quantified by measuring absorbance at OD_{595} (B).

mutations in *icaR* and *tcaR.* OD_{600} was measured while strains were grown micro-aerobically in TSB at 37°C. In 1457, the *tcaR* and *icaR tcaR* mutants exhibited lower growth rate during exponential phase than wild type (Figure 3.3). Since these strains also displayed increased PIA synthesis and biofilm formation, it is likely this process is energetically unfavorable. Since PIA synthesis occurs when the TCA cycle is inactive and involves funneling of carbon away from glycolysis and cell wall synthesis, it is reasonable to postulate that decreased cell growth in these mutants is due to enhanced PIA synthesis. However, complementation with constitutively expressing *tcaR* only slightly increased growth rate although PIA synthesis was completely repressed (Figure 3.2). Since *tcaR* is normally expressed at constitutively low levels (158), this suggests that high *tcaR* expression can also negatively impact growth, perhaps due to altered expression of other genes in the TcaR regulon. In contrast, growth defects were not observed in the mutants of CSF41498 with the exception that CSF41498 Δ*icaR* did not reach similar growth yield as wild type (Figure 3.3). Since this mutant exhibited increased PIA synthesis (Figure 3.2), this could be a result of altered carbon flux towards PIA synthesis as well as increased cell clumping. Notably, the $_{OD600}$ of many strains began to drop around hour 7 due to accumulation of PIA synthesis, which would result in aggregation of cells.

Biofilm formation is more robust in 1457 Δ*tcaR*. To further investigate the effects of deleting *icaR* and *tcaR* on biofilm formation, we used the BioFlux microfluidics system and automated image acquisition technology to monitor biofilm formation. The plasmid pNF206, carrying a P*ica*::GFP reporter, was used to monitor *icaADBC* expression however, this is not an accurate indication of *ica* expression as biofilms grow in multiple layers, affecting the relative levels of fluorescence detected. Analysis of biofilm formation revealed that 1457 Δ*tcaR* and 1457 Δ*icaR* Δ*tcaR* began aggregating and forming towers sooner compared to wild type and Δ*icaR* (Figure 3.4). Additionally, biofilm formation was more robust in 1457 Δ*tcaR*

and 1457 Δ*icaR* Δ*tcaR.* While a small increase in biofilm formation was observed in 1457 Δ*icaR* compared to wild type, the differences observed in 1457 Δ*tcaR* and 1457 Δ*icaR* Δ*tcaR* were more apparent. Overall, these data showed that inactivation of *tcaR* enhances biofilm formation and confirmed our findings that TcaR is the major repressor of *icaADBC* and biofilm formation in 1457.

IcaR is the primary repressor in clinical isolates 7613 and 9958. Our results thus far illustrate a difference in IcaR and TcaR regulation of *icaADBC* and PIA synthesis between 1457 and CSF41498. To investigate whether this is strain specific, other clinical isolates of *S. epidermidis* were assessed. Two genetically amenable and low PIA producing clinical isolates (CSF41498-like) were identified and *icaR* and *tcaR* mutations were generated by transduction from 1457 Δ*icaR* and 1457 Δ*tcaR,* respectively. Similar to observations made in CSF41498, increased *icaA* transcription was detected in the *icaR* mutants of 7613 and 9958 while no difference was observed with the *tcaR* mutants (Figure 3.5). This transcriptional data was corroborated by static biofilm assays showing only increased biofilm formation in the *icaR* mutants, not Δ*tcaR*. Unfortunately, we were unable to generate *icaR* and *tcaR* mutations in high PIA producing strains (such as 8595 and 8889) via transduction or allelic exchange methods. Experiments performed with these mutants would confirm whether high PIA producing strains were regulated by TcaR, in a manner similar to 1457 (as opposed to low PIA producing strains such as CSF41498).

***icaR* transcription varies among *S. epidermidis* clinical isolates**. As we have previously observed, when *icaR* and *tcaR* are expressed in single-copy using a constitutive promoter (P_{sarA}),

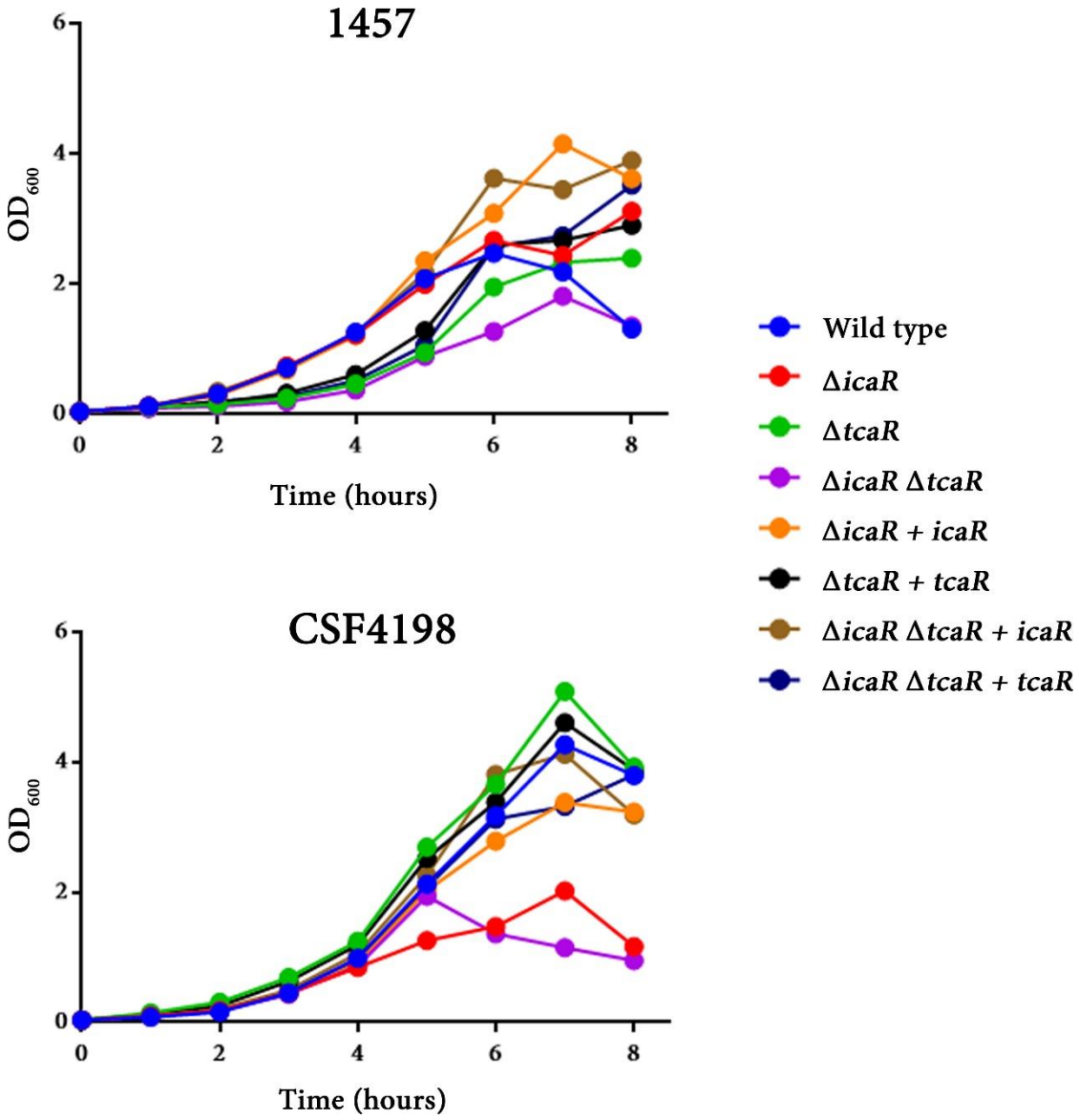

Figure 3.3. Alterations in *tcaR* expression affects growth. Microaerobic growth was assessed by measuring OD_{600} hourly. 1457 Δ*tcaR*, 1457 Δ*icaR* Δ*tcaR,* 1457 Δ*tcaR* + *tcaR*, 1457 Δ*icaR* Δ*tcaR* + *tcaR* showed lower exponential growth rates compared to 1457 wild type. CSF41498 strains all grew at similar rates although CSF41498 Δ*tcaR* and CSF41498 Δ*tcaR + tcaR* grew slightly better.

Figure 3.4. Biofilm formation is more robust in 1457 Δ*tcaR* and 1457 Δ*icaR* Δ*tcaR*. Strains carrying P*ica::*GFP reporter (pNF206) were grown in 50% TSB in the BioFlux Microfluidic system for 18 hours at 37°C. Images were taken with an automated image acquisition system and video stills were captured at the indicated time points after inoculation. Biofilm formation in 1457 Δ*icaR* was slightly increased compared to 1457 wild-type. However, 1457 Δ*tcaR* and 1457 Δ*icaR* Δ*tcaR* began forming microcolonies sooner and the biofilms were more robust by 10 hours compared to 1457 wild-type and 1457 Δ*icaR*.

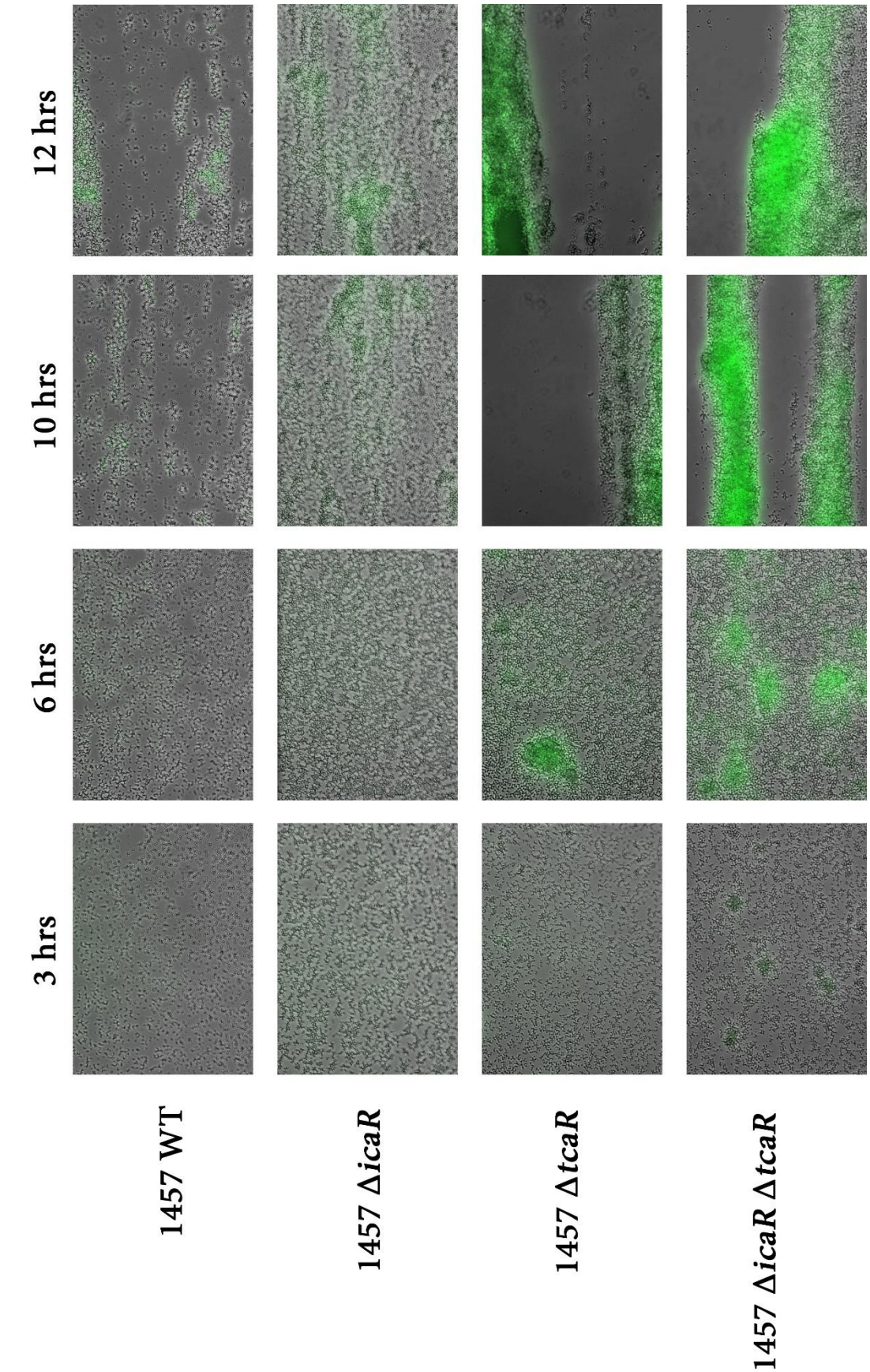
3 hrs
6 hrs
10 hrs
12 hrs
1457 WT
1457 ΔicaR
1457 ΔtcaR
1457 ΔicaR ΔtcaR

icaA transcription and PIA synthesis were completely repressed (Figure 3.2), indicating that IcaR and TcaR are fully functional as repressors of *ica*. Therefore, we hypothesized that inactivating *icaR* in 1457 had no effect due to already low or no *icaR* transcription. Northern blot analysis confirmed that less *icaR* transcript was detected in 1457 compared to CSF41498 (Figure 3.5). To determine whether this is strain specific, we examined other *S. epidermidis* clinical isolates to investigate whether variation in PIA synthesis is determined by *icaR* expression (as it seems to be in 1457 and CSF41498). 7613 and 9958 are both low PIA producing strains however, low *icaR* transcript was detected in isolate 9958 while high *icaR* transcript was detected in 7613. This suggests that *icaR* transcription is not the only determining factor as to whether a strain is high or low PIA producing. Nevertheless, our transcriptional data show that, in 1457, TcaR is the major repressor due to the absence of *icaR* expression. However, expression of *icaR* does not determine whether a strain is a high or low PIA producer.

IcaR expression is higher in 1457 biofilm compared to CSF41498. To determine whether *icaR* transcription levels correspond to IcaR protein levels, we planned to perform western blot analyses. To this end, recombinant IcaR proteins were sent to Cocalico Biologicals, Inc. (Stevens, PA) for production of custom polyclonal antibodies specific for recombinant IcaR. After boosting with IcaR antigen three times, the serum was tested using cell lysates collected from 1457 and CSF41498 wild-type and *icaR* mutants grown for 2, 4, 6, 8, 10, and 12 hours micro-aerobically. While the appropriately sized band for recombinant IcaR protein control was observed on a western blot, no bands were observed with the cell lysates (data not shown). A final boost was performed with recombinant IcaR conjugated to hemocyanin since hemocyanin is known to elicit

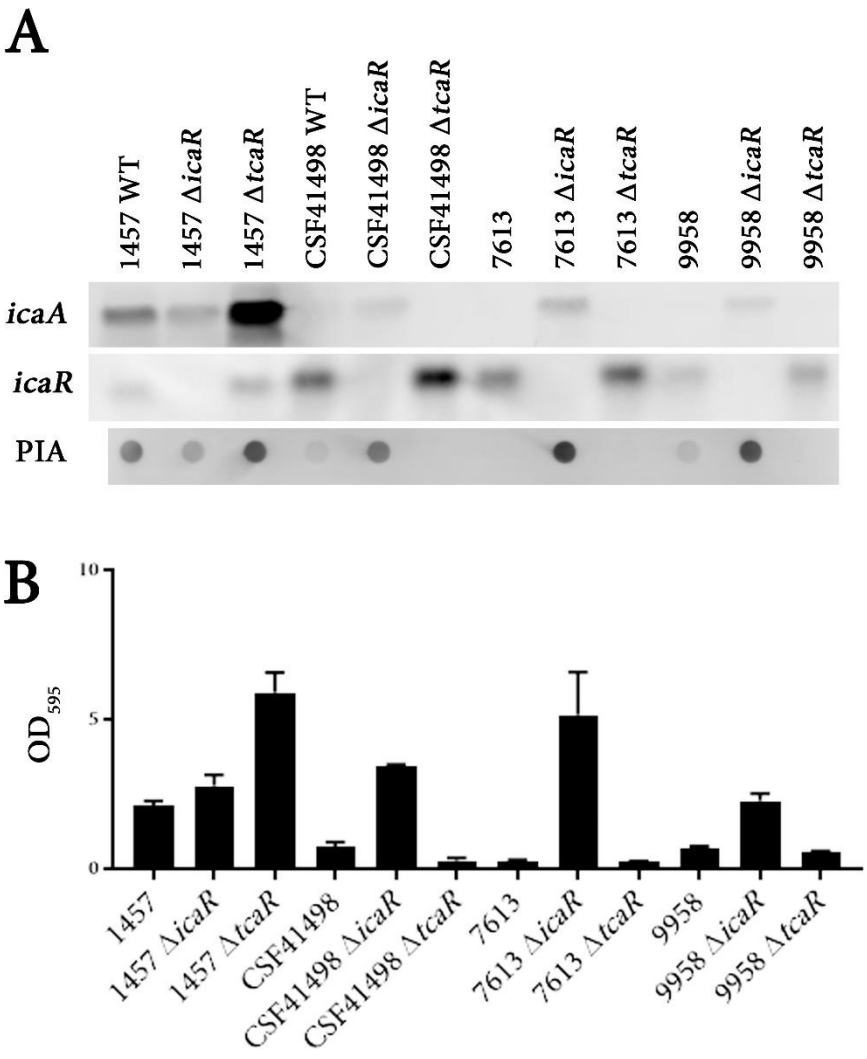

Figure 3.5. Clinical isolates 7613 and 9958 are regulated by IcaR. Increased *icaA* transcription, PIA synthesis, and biofilm were detected in 7613 Δ*icaR* and 9958 Δ*icaR*. However, no change was observed in the *tcaR* mutants. *icaR* and *tcaR* mutations were generated by transduction from 1457 Δ*icaR* and Δ*tcaR.* RNA was collected at mid-exponential phase, PIA was isolated from post-exponential phase, and biofilm was assessed by crystal violet staining after 24 hours of growth in TSB.

culture (data not shown). However, when grown in 6-well plates, biofilms collected at 38 hours yielded the

appropriately sized bands using anti-IcaR serum. At 38 hours, 1457 expressed less IcaR compared to CSF41498 (Figure 3.6). The presence of correct sized protein bands in biofilms constitutively expressing *icaR*, but not *tcaR*, as well as a band in the purified IcaR lane suggested the serum was specific for IcaR. However, the band in the purified IcaR lane ran higher than bands from lysates. Additionally, there was a faint band in the purified TcaR lane and nonspecific bands at the top of the blot, especially around 40 kDa, suggesting non-specificity with the anti-IcaR serum. To address this, the anti-IcaR serum was affinity purified using recombinant IcaR protein bound to AffiGel 10 (Bio-Rad). Purified anti-IcaR serum resulted in a blank blot (not shown) suggesting that the serum does not contain anti-IcaR antibodies. At this point, we concluded that we were unsuccessful in generating IcaR-specific polyclonal antibody. However, preliminary western blot analysis with lysate collected from a 38-hour biofilm seemed to suggest that IcaR levels are lower in 1457 compared to CSF41498, confirming our transcriptional data (Figure 3.5).

TcaR binds to multiple sequences in the *icaR-icaA* intergenic region. Previous reports have demonstrated that IcaR binds to a sequence directly upstream of the *icaA* start site and TcaR could bind to three different sites containing a 33-bp pseudopalindromic sequence (Figure 1.1) (111). Of the three putative sites, the one proposed to bind with the highest affinity is located very close to the IcaR binding site, suggesting IcaR and TcaR may be competing for binding to the *ica* promoter. To determine whether TcaR can bind directly to the *icaR-icaA* intergenic region, recombinant proteins were purified and electrophoretic mobility shift assays (EMSA) were performed. As IcaR is known to bind to the *icaR-icaA* intergenic region, recombinant IcaR was

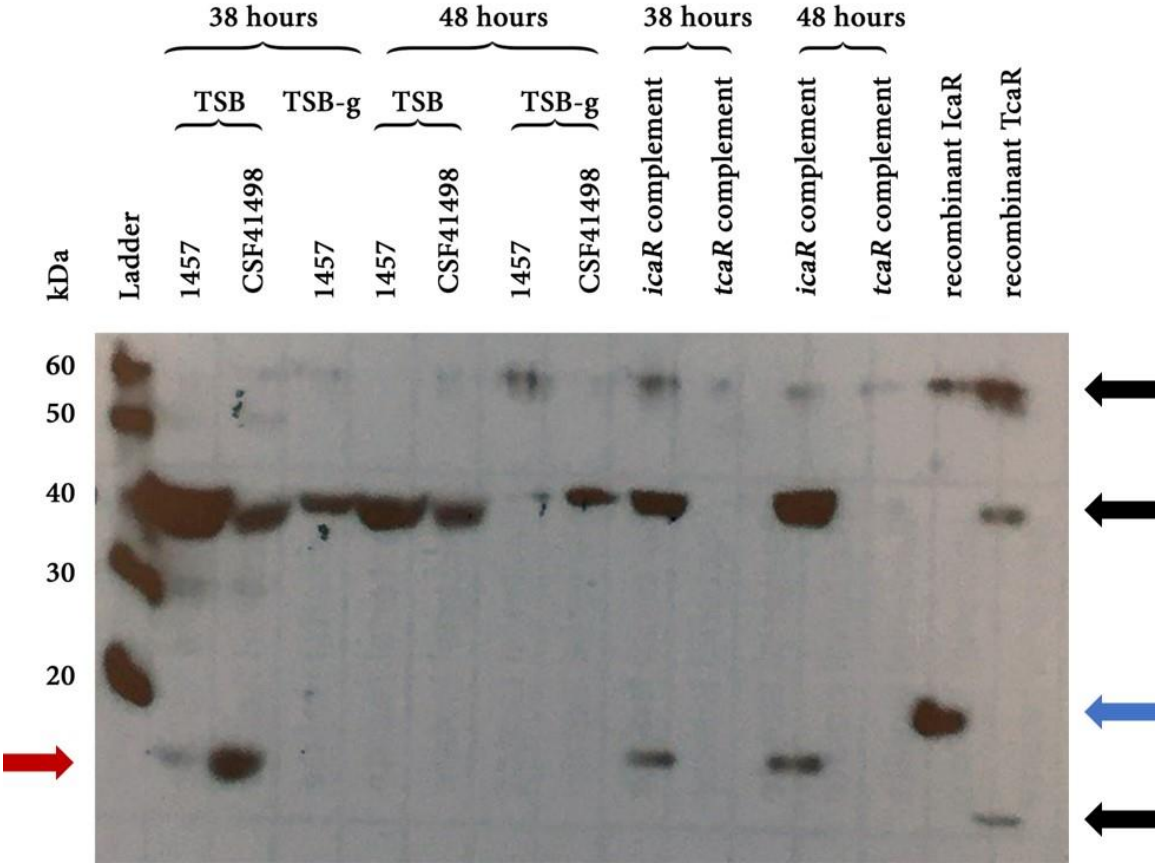

Figure 3.6. IcaR levels are higher in CSF41498 biofilms than 1457. Cell lysates were collected from biofilms grown in TSB and TSB without glucose. At 38 hours post-inoculation, higher IcaR expression was detected in CSF41498 biofilms compared to 1457. No IcaR was detected in 12-hour, 24-hour (not shown), 38-hour biofilms grown without glucose and 48-hour biofilms. Complementation with *icaR* resulted in same sized bands as 1457 and CSF41498 wild-types (red arrow). However, recombinant IcaR control showed a larger sized product (blue arrow). Non-specific bands are indicated by black arrows.

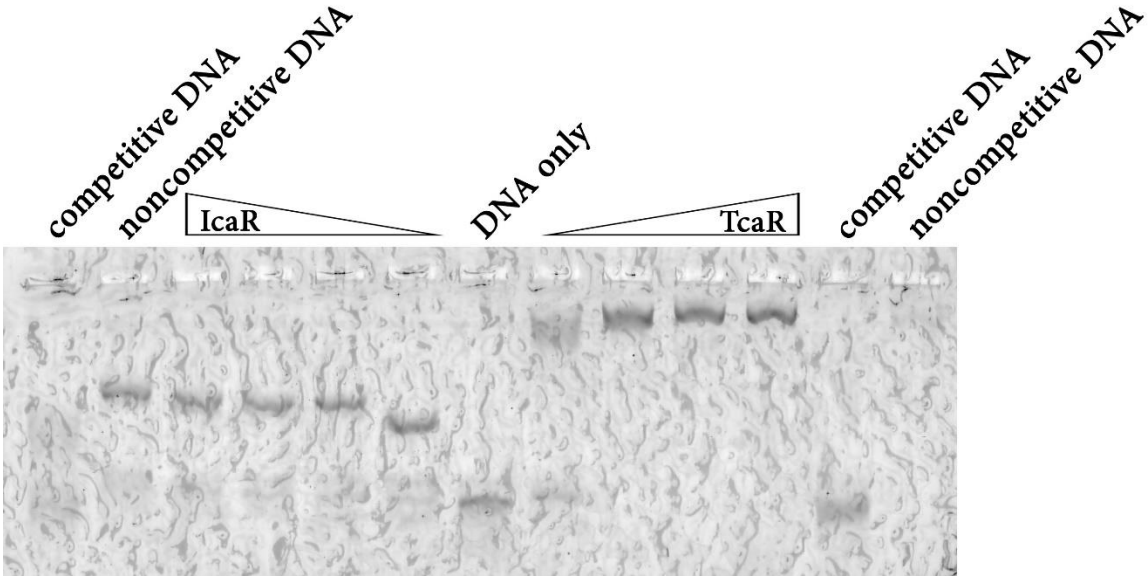

Figure 3.7. Recombinant IcaR and TcaR can bind to the *ica* promoter. Recombinant IcaR and TcaR were incubated with double-stranded fluorescein-labeled *ica* promoter DNA (PCR amplified) at room temperature for 30 minutes then electrophoresed on a 6% polyacrylamide gel under non-denaturing conditions. Noncompetitive DNA is salmon sperm DNA and competitive DNA is non-fluorescein-labeled *ica* promoter DNA. Addition of IcaR and TcaR resulted in a shift in DNA migration that can be abolished by competitive DNA.

purified and used as a control. Indeed, incubation of increasing concentrations of IcaR with *icaR-icaA* intergenic DNA resulted in decreased DNA migration compared to the DNA only control, which is a result of DNA movement being hindered by binding of IcaR (Figure 3.7). Similarly, the addition of increasing concentrations of TcaR also resulted in decreased mobility of DNA although the shift is bigger compared to IcaR suggesting that binding of TcaR resulted in a bulkier product than binding with IcaR. This is in agreement with crystal structure studies showing that IcaR bound to DNA as two dimers while TcaR complexed with DNA as a heptamer (108, 157). These interactions were direct as addition of noncompetitive DNA (Salmon sperm DNA) did not affect the shift in contrast to the addition of unlabeled competitive DNA. Thus, these data confirm that IcaR and TcaR bind directly to the *S. epidermidis icaR-icaA* intergenic region (108, 111).

Next, DNase I footprinting assays were performed to determine if IcaR and TcaR bind to similar DNA sequences within the *icaR-icaA* intergenic region. As expected, binding of IcaR to the DNA resulted in a protected region just upstream of the *icaA* start site (Figure 3.8) confirming previous DNase I footprinting results that IcaR bound to a 42 bp sequence in the *ica* promoter (107). Interestingly, the addition of TcaR resulted in a large protected zone covering most of the *icaR-icaA* intergenic region, including the *icaR* promoter and the IcaR binding site. These data are in agreement with previous studies demonstrating that TcaR binds to multiple sites containing a 33 bp pseudopalindromic consensus sequence (111, 112). Taken together, these data show that TcaR binds to multiple sites within the *icaR-icaA* intergenic region and may bind to similar regions as IcaR.

TcaR is a repressor of *icaR*. DNase I footprinting assay showed that TcaR bound to multiple sites in the *icaR-icaA* intergenic region, including within the *icaR* promoter suggesting

Figure 3.8. TcaR binds to multiple sites in the *icaR-icaA* intergenic region. P^{32}-labeled *ica* promoter DNA was incubated with increasing concentrations of recombinant IcaR or TcaR. Incubation with IcaR resulted in a footprint upstream of *icaA.* Incubation with TcaR resulted in multiple footprints throughout the intergenic region (noted on right side of the figure). Previously proposed IcaR and TcaR binding sites are noted on the left side of the figure.

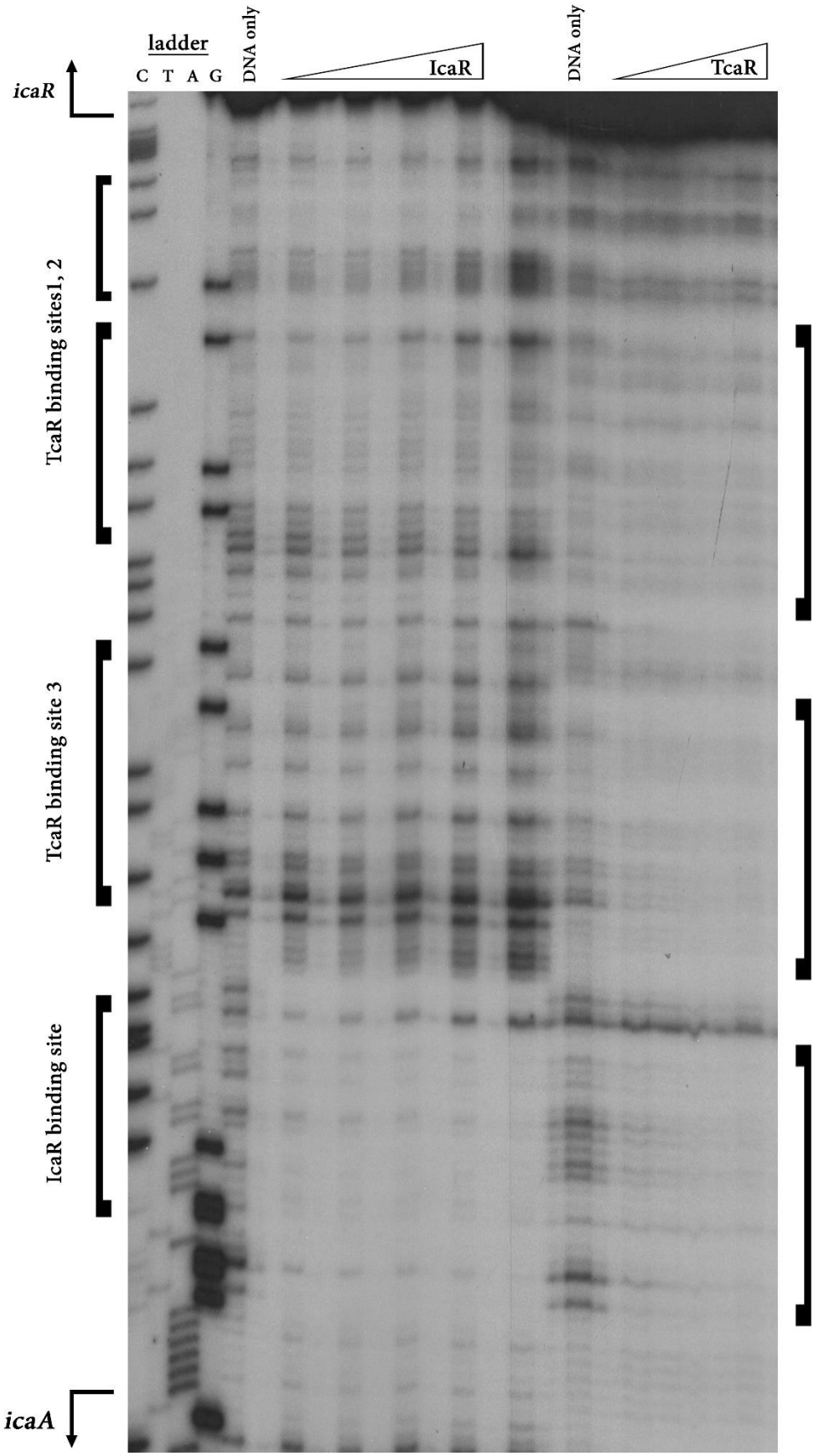
ladder
C T A G
DNA only
IcaR
DNA only
TcaR
icaR
TcaR binding sites1, 2
TcaR binding site 3
IcaR binding site
icaA

that TcaR may regulate *icaR* transcription. To investigate this, qRT-PCR was performed with *icaR* specific primers using RNA isolated from 1457 and CSF41498 wild types and *tcaR* mutants. Indeed, *icaR* transcription was approximately 5-fold higher in the *tcaR* mutants of 1457 and CSF41498 compared to wild-type (Figure 3.9) suggesting that TcaR not only functions as a repressor of *icaADBC* transcription but can also repress *icaR.* This provides multiple ways in which TcaR can regulate *icaADBC* and adds to the complexity of PIA regulation in *S. epidermidis.*

Mutations can be generated to alter PIA synthesis in 1457 and CSF41498. Previous studies have hypothesized that mutations which facilitate enhanced PIA synthesis are selected to allow for colonization in high shear niches such as the lumen of a catheter (48, 90). Based on our data with 1457, it is possible that some of these mutations result in decreased *icaR* transcription, de-repression of *icaADBC* and increased PIA synthesis. Therefore, we set out to isolate CSF41498 mutants that exhibit increased PIA synthesis and 1457 mutants that produce less PIA than wild type.

To identify potential mutations that mediate increased PIA synthesis, CSF41498 was grown in tissue culture flasks and the media was replaced daily for five days. On the fifth day, the resulting biofilm was collected, dispersed and plated on Congo Red agar (CRA). CRA was used to identify CSF41498 mutants with enhanced PIA synthesis since high PIA producing colonies appear crusty instead of smooth on this medium (Figure 3.10A) (155).

A total of ten CSF41498 mutants with increased PIA and biofilm formation were isolated and six were selected for further analysis. We observed highly variable phenotypes with all six of these mutants in regard to *icaA* and *icaR* transcription and PIA and biofilm synthesis (Figure 3.10).

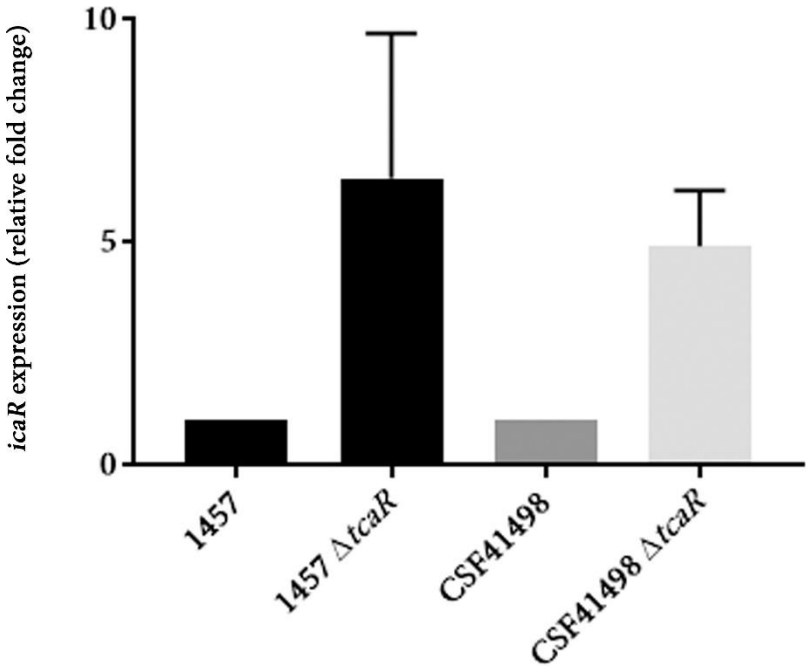

Figure 3.9. TcaR represses *icaR* transcription. *icaR* expression is increased in 1457 Δ*tcaR* and CSF41498 Δ*tcaR* compared to the wild-types. RNA was collected from mid-exponential phase of microaerobic growth and qRT-PCR was performed with *icaR* specific primers. Expression was determined by quantification of SYBR-green fluorescence, normalized to *gyrB* levels, and relative expression was calculated based on wild-type expression levels.

Enhanced *icaA* transcription was detected in all six mutants and all displayed increased biofilm and PIA synthesis (with the exception of P4). Based on our observations with 1457, we expected that some of the mutants would display decreased *icaR* expression. Indeed, less *icaR* transcript was detected in mutants P4 and O7. Of particular interest was mutant O7 as it displayed the most similar phenotype to 1457. No *icaR* was detected in mutant O7 and a more pronounced biofilm and PIA phenotype was observed in the *tcaR* mutant compared to the *icaR* mutant. Interestingly, mutants A9, P4, D9, N2, and O7 had decreased *icaA* transcription when *icaR* and *tcaR* mutations were introduced in this mutant background suggesting that the function of IcaR and TcaR with regards to the regulation of *icaADBC* has been altered in these mutants. Unfortunately, for unknown reasons, we were unable to generate *tcaR* mutations in mutants A9 or P4 by either Φ71 and ΦA6C mediated transduction or direct allelic replacement methodologies.

To identify 1457 mutants that produce decreased PIA, 1457 was grown in Stovall flow cells and plated on CRA to isolate smooth colonies as previously described (48), generating mutants PV18, PV19, PV21, and PV22. In addition, 1457 smooth mutants were isolated from a guinea pig tissue cage model as previously described (159), generating 22R5 and 22R6. With the exception of PV22, *icaA* transcription was markedly lower in these mutants compared to 1457 wild type confirming these mutants carry mutations that repress transcription of *icaADBC*. In addition, outside of strain 22R6, which appeared to produce similar amounts of PIA as 1457, PIA immunoblot and biofilm assay corroborated this observation indicating that these isolates produce less PIA-mediated biofilm (Figure 3.11A, B). Importantly, other than PV22, all 1457 mutants had similar phenotypes as CSF41498 (compared to 1457 wild type) including enhanced *icaR* transcript, decreased *icaA* transcript, and increased biofilm and PIA synthesis as well as an increase in *icaA* transcript in the *icaR* mutants.

Aside from a modest increase in PIA production, little phenotype was observed in the *tcaR* mutants. Interestingly, *icaA* transcription does not correlate with PIA synthesis and biofilm in mutant PV22, however, allelic replacement of *icaR* does result in increased PIA synthesis and biofilm formation. Together, these experiments using both CSF41498 and 1457 suggest that mutations can be easily selected that will result in altered *icaR* transcription, PIA synthesis, and biofilm formation. This suggests that *S. epidermidis* can fine tune the regulation of *icaADBC* by acquiring mutations that alter expression of *icaR.*

Whole genome sequencing was performed to identify the location of the mutations in the ten CSF41498 mutants and six 1457 mutants that were isolated. First, it is important to note that multiple mutations were detected in all strains sequenced. In the 1457 mutants, we found mutations in several genes (Table 3.1) including ferrous iron transporter B (*feoB*), tributyrin esterase, phosphoenolpyruvate synthase regulatory protein, ribonuclease Y, as well as two hypothetical proteins with unknown function. Not surprisingly, we also discovered mutations in *icaA* (in PV22) and σ^B (PV19). As previously discussed, σ^B activates *icaADBC* by indirectly repressing *icaR* expression (105) therefore, mutations in either *icaA* or σ^B could lead to abolishment of *icaADBC* transcription and PIA synthesis.

Results from sequencing the ten CSF41498 mutants revealed that each carried mutations in multiple genes (Table 3.2). Mutations that were identified in multiple isolates include homoserine-*O*-acetyltransferase, aldehyde dehydrogenase A (*aldA*), c-di-AMP phosphodiesterase (*gdpP*), L-carnitine/choline transporter (*opuCA*), respiratory nitrate reductase (*narH*), and an Abr

family transcriptional regulator. Unsurprisingly, we also discovered mutations in *icaB* and *icaR.* The enzyme IcaB is a deacetylase whose function is to impart a negative charge on PIA, allowing for interaction with the cell surface as well as to various surfaces. Surprisingly, a mutation in *icaB* was identified in mutant O7 although *icaA* transcript and PIA synthesis were higher compared to CSF41498 wild type, suggesting that this substitution mutation has resulted in enhanced IcaB activity. As expected, a mutation in *icaR* would lead to de-repression of *icaADBC,* and thus PIA synthesis and biofilm formation. Since there are multiple mutations in these isolates, it is likely altered *icaADBC* expression and PIA synthesis are a result of multiple mutations. Furthermore, many mutations result in substitutions within their gene products, therefore the effects on protein function is largely unknown.

Aside from *icaR*, sequencing results identified one other transcriptional regulator potentially involved in regulation of *icaADBC*. In *B. subtilis,* AbrB regulates two genes implicated in biofilm formation: *yoaW* and *sipW*. SipW was shown to be a signal peptidase with function in processing either an intercellular adhesin or motility structure (160, 161). Considering this, the regulator we identified may also function to regulate biofilm formation in staphylococci. However, further experiments are required to confirm this.

Additionally, the gene encoding for PEP synthase regulatory protein was also mutated. The synthase enzyme functions to convert pyruvate to PEP during gluconeogenesis. PIA synthesis is partially regulated by metabolism and studies investigating this have shown that *icaADBC* transcription can be controlled by regulators responding to the metabolic state of the cell (91). For this reason, any changes to cellular metabolism, including gluconeogenesis, may affect function of

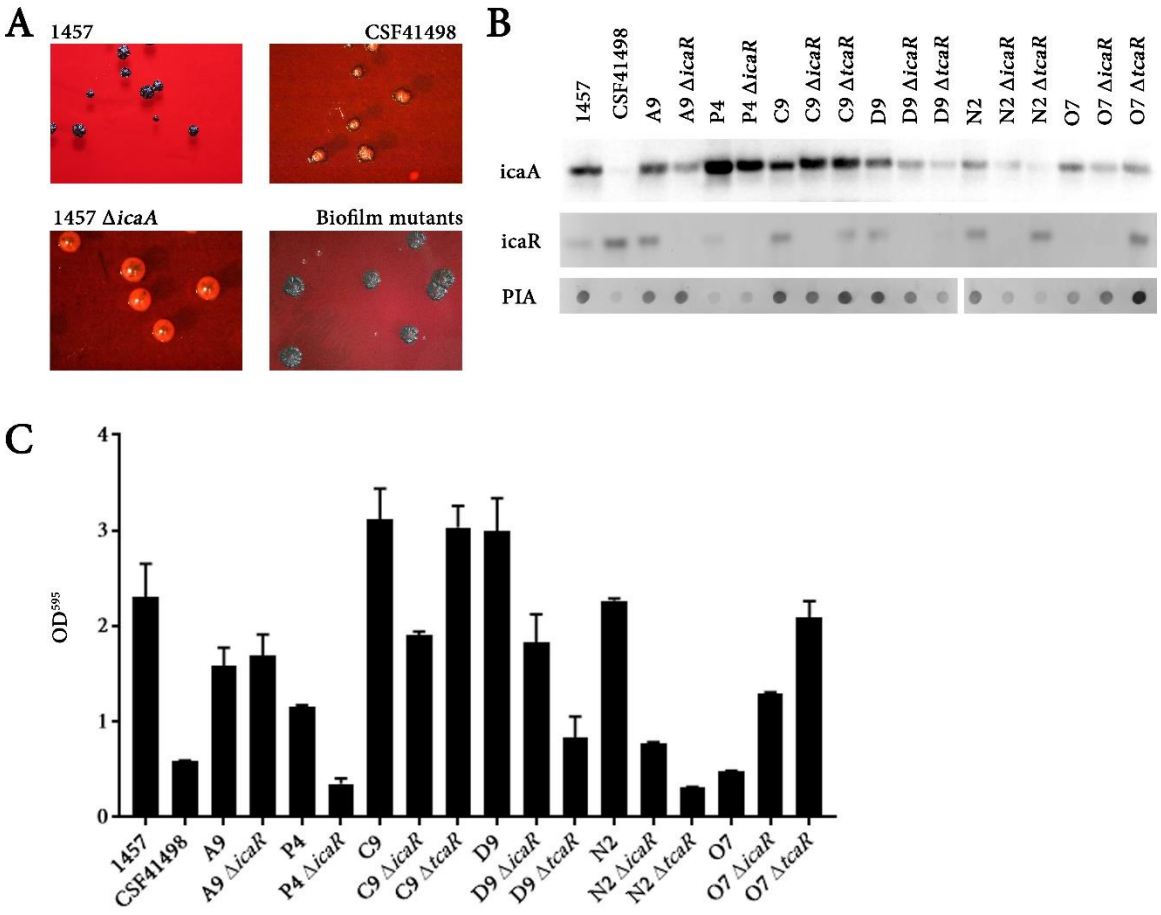

Figure 3.10. CSF41498 biofilm mutants express more *icaA* transcription. CSF41498 mutants were screened on Congo red agar (CRA) for increased PIA synthesis. Strains not synthesizing PIA (such as 1457 Δ*icaA*) have a smooth, round morphology on CRA while strains synthesizing high amounts of PIA (such as 1457) are crusty and rough in appearance. CSF41498 makes low amounts of PIA and so have a phenotype in between 1457 and 1457 Δ*icaA*. CSF41498 biofilm mutants appeared more crusty and rough on CRA than CSF41498 wild-type (A). CSF41498 biofilm mutants showed increased *icaA* transcription (B), PIA synthesis (B), and biofilm formation (C) compared to CSF41498 wild-type. Introduction of *icaR* and *tcaR* mutations in these mutants did not result in higher *icaA* transcription, PIA synthesis, or biofilm formation. Compared to CSF41498 wild-type, mutants P4, D9, N2, and O7 expressed lower levels of *icaR* transcription (B).

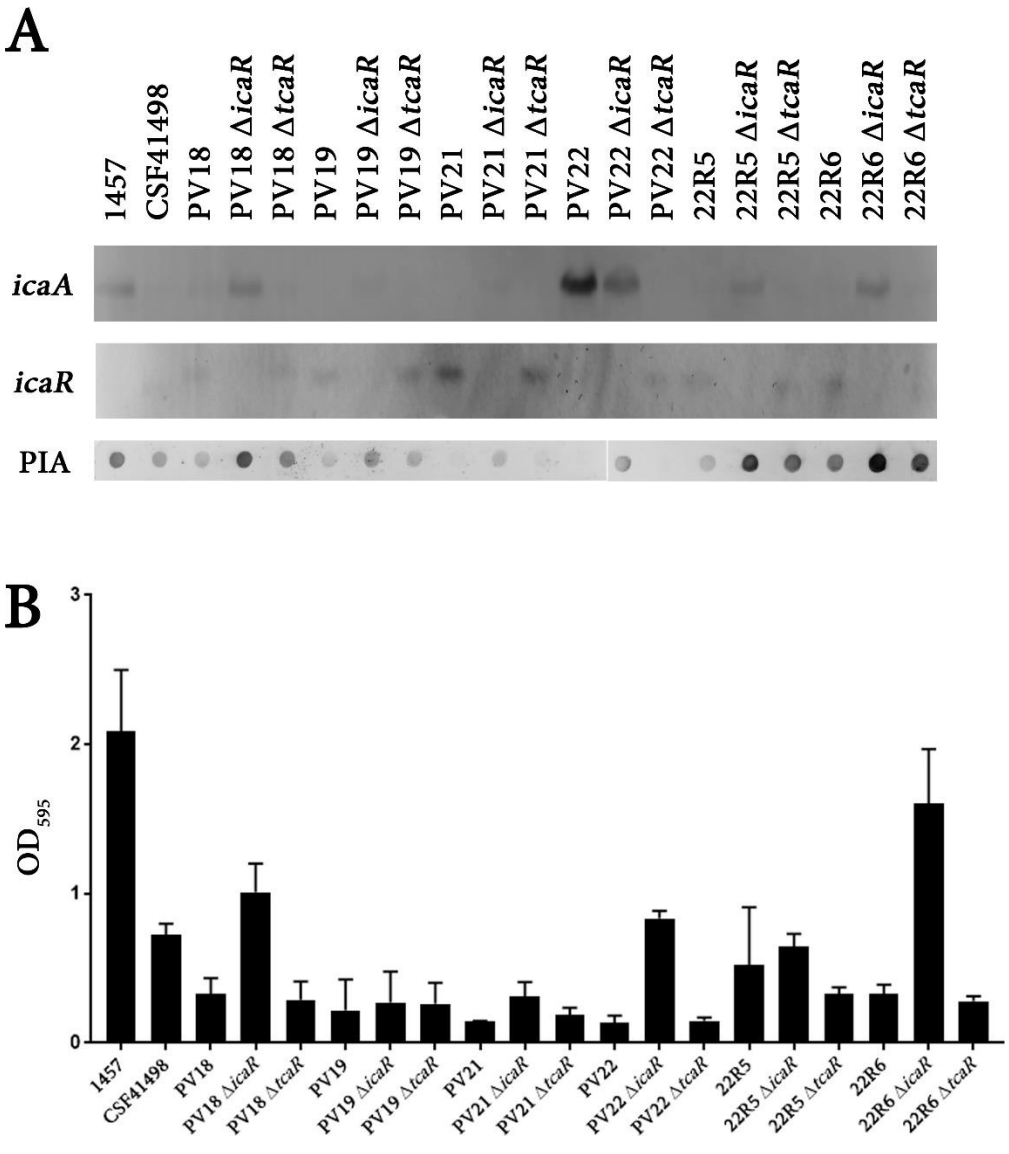

Figure 3.11. 1457 biofilm mutants exhibit lower *icaA* transcription and PIA synthesis than wild-type. Less *icaA* transcript, PIA, (A) and biofilm (B) were detected in biofilm mutants compared to 1457. Although less biofilm and PIA synthesis were detected in PV22, enhanced *icaA* transcript was detected. Increased *icaR* transcription (A) was detected in 1457 biofilm mutants, similar to CSF41498 (A).

these regulators, leading to altered *icaADBC* transcription. However, additional studies are required to determine whether PEP synthase and its regulator have any effect on *icaADBC* transcription.

Finally, our sequencing results also identified two ribonucleases: ribonuclease Y (RNase Y) and ribonuclease Z (RNase Z). Due to their roles in regulating mRNA stability, it is likely that altering the function of these ribonucleases would affect mRNA levels of *icaADBC* or one of its regulators, resulting in either increased or decreased *icaADBC* transcript. For example, Ruiz de los Mozos et al. showed that interaction between the *icaR* 3′-UTR and 5′-UTR forms a double-stranded region targeted by RNase III, resulting in degradation of the *icaR* mRNA (162).

GdpP is not a regulator of *icaADBC.* GGDEF domain-containing proteins have diguanylate cyclase activity (and sometimes phosphodiesterase activity) (163, 164). GdpS is the only staphylococcal protein carrying this highly conserved domain while GdpP has a modified domain (165). GdpP has been shown to modulate biofilm formation in several organisms (166-169) and GdpS can regulate PIA synthesis by increasing *icaADBC* mRNA levels in *S. epidermidis* (165). Since *gdpP* was mutated in multiple CSF41498 mutants, we speculated that GdpP has function in regulating *icaADBC* and PIA synthesis. To investigate whether inactivating *gdpP* would lead to decreased *icaADBC* transcription, *gdpP* mutants were generated in 1457 and CSF41498 using allelic replacement methodologies. No changes in *icaA* transcription and biofilm formation were observed in the *gdpP* mutants of both 1457 and CSF41498 (Figure 3.12), indicating that GdpP, alone, does not function in regulating PIA in *S. epidermidis*. While mutations in *gdpP* did arise in multiple CSF41498 biofilm mutants, it must be noted that these were substitution mutations. It is unknown what effects these substitutions have, if any, on protein function. Furthermore, the biofilm mutants carried mutations in multiple genes suggesting that increased PIA synthesis could be due to a

combination of multiple factors. Further studies are required to determine which of the remaining identified genes, or combination of genes, function in regulation of PIA synthesis.

Using a *lacZ* reporter to identify regulators of *icaADBC*. In addition to generating random mutations exhibiting altered *icaADBC* expression, we also proposed a more direct method to identify regulators of *icaADBC*. The mariner transposon *bursa aurealis* will be used to target non-essential genes of the *S. epidermidis* genome. By generating this library in a reporter strain carrying *lacZ* fused to the promoter of *icaADBC*, a blue/white screen can be used to distinguish high *icaADBC* expressing cells from low. In this way, we will be able to identify all mutants that have altered *icaADBC* transcription, narrowing down candidates involved in the regulation of *icaADBC* and PIA. We successfully generated P*ica::lacZ* reporters in *S. epidermidis* 1457 and CSF41498 by cloning this construct into *icaADBC*, rendering the operon nonfunctional. To demonstrate that the *lacZ* reporters were working as intended, they were grown in TSB supplemented with increasing concentrations of NaCl and β-galactosidase activity was measured. Our results showed that β-galactosidase activity is undetectable in 1457 and CSF41498 wild-types. However, in the reporters, β-galactosidase activity, and therefore *icaADBC* expression, was higher in TSB supplemented with NaCl compared to TSB alone. In 1457, 4% NaCl was optimal for induction of *icaADBC* while CSF41498 was equally induced in 2% and 4% NaCl (Figure 3.12). Since these results are aligned with previous observations that *icaADBC* transcription is higher in 1457 and can be induced by NaCl (Figure 3.2, 3.5) (88, 105, 118), these data confirm that our *lacZ* reporters were appropriately constructed and can be used to assess *icaADBC* expression.

Table 3.1 Genes mutated in CSF41498 biofilm mutants

Mutant	Product	GenBank gene	Mutation location	Amino Acid Change	Protein Effect
C9	c-di-AMP phosphodiesterase	*gdpP*	18,915	R -> S	Substitution
	Aldehyde dehydrogenase A (EC 1.2.1.22)	*aldA*	474,625	T -> P	Substitution
	Aldehyde dehydrogenase A (EC 1.2.1.22)	*aldA*	474,628	-C	Frame Shift
	Respiratory nitrate reductase beta chain (EC 1.7.99.4)	narH	577,776	K -> I	Substitution
	IS110 family transposase		701,051-702,610		Complete deletion
P4	Osmosensitive K+ channel histidine kinase (EC 2.7.3.-)	*kdpD*	45,927	G -> V	Substitution
	Biofilm operon *icaABCD* HTH-type negative transcriptional regulator	*icaR*	241,635		Truncation
	Aldehyde dehydrogenase A (EC 1.2.1.22)	*aldA*	474,625	T -> P	Substitution
	Aldehyde dehydrogenase A (EC 1.2.1.22)	*aldA*	474,628	-C	Frame Shift
	FUSC family protein		488,318	T -> A	Substitution
	Respiratory nitrate reductase beta chain (EC 1.7.99.4)	*narH*	577,776	K -> I	Substitution
	c-di-AMP phosphodiesterase	*gdpP*	18,910	R -> L	Substitution
	IS110 family transposase		701,051-702,610		Complete deletion
A9	Cadmium resistance protein		321,101		Truncation
	2',3'-cyclic-nucleotide 2'-phosphodiesterase (EC 3.1.4.16)		1,855,292	A -> T	Substitution
	c-di-AMP phosphodiesterase	*gdpP*	19,338	Y -> N	Substitution
	IS110 family transposase		701,051-702,610		Complete deletion
D9	Ornithine carbamoyltransferase (EC 2.1.3.3)	*argF*	176,852	G -> C	Substitution
	Aldehyde dehydrogenase A (EC 1.2.1.22)	*aldA*	474,625	T -> P	Substitution

	Respiratory nitrate reductase beta chain (EC 1.7.99.4)	*narH*	577,776	K -> I	Substitution
	replication protein	*repL*	1,809,378	A -> T	Substitution
	ATP-dependent sacrificial sulfur transferase	*larE*	2,206,310	G -> S	Substitution
	IS110 family transposase		701,051-702,610		Complete deletion
O7	Polysaccharide intercellular adhesin (PIA) biosynthesis deacetylase	*icaB*	238,971	L -> F	Substitution
	site-specific integrase (promoter)		1,811,994	G -> C	
	IS110 family transposase		701,051-702,610		Complete deletion
L1	c-di-AMP phosphodiesterase	*gdpP*	18,919	A -> G	Substitution
	Aldehyde dehydrogenase A (EC 1.2.1.22)	*aldA*	474,625	T -> P	Substitution
	Aldehyde dehydrogenase A (EC 1.2.1.22)	*aldA*	474,628	-C	Frame Shift
	Respiratory nitrate reductase beta chain (EC 1.7.99.4)	*narH*	577,776	K -> I	Substitution
	Glycyl-tRNA synthetase (EC 6.1.1.14)		1,251,243		None
	IS110 family transposase		701,051-702,610		Complete deletion
H5	c-di-AMP phosphodiesterase	*gdpP*	18,475	P -> R	Substitution
	homoserine-o-acetyltransferase		167,111	A -> S	Substitution
	Osmotically activated L-carnitine/choline ABC transporter, ATP-binding protein	*opuCA*	168,980		Frame Shift
	IS110 family transposase		701,051-702,610		Complete deletion
J2	3-methyl-2-oxobutanoate hydroxymethyltransferase (EC 2.1.2.11)	*panB*	401,117	N -> K	Substitution
	Ferredoxin-dependent glutamate synthase (EC 1.4.7.1)		519,910	R -> L	Substitution
	dynamin family protein		1,364,423		Truncation
	Methionyl-tRNA formyltransferase (EC 2.1.2.9)		1,642,814	G -> V	Substitution

	IS110 family transposase		701,051-702,610		Complete deletion
E8	AbrB family transcriptional regulator		1,164,119	V -> L	Substitution
	Hypothetical protein SAV1801		2,000,182		Frame Shift
	IS110 family transposase		701,051-702,610		Complete deletion
N2	homoserine-o-acetyltransferase		167,111	A -> S	Substitution
	Osmotically activated L-carnitine/choline ABC transporter, ATP-binding protein OpuCA		168,980		Frame Shift
	Biofilm operon icaABCD HTH-type negative transcriptional regulator	*icaR*	241,492	A -> D	Substitution
	Multidrug resistance protein B		768,989	L -> I	Substitution
	Ammonium transporter		887,720	H -> D	Substitution
	UDP-N-acetylmuramate--alanine ligase (EC 6.3.2.8)		1,081,411	G -> E	Substitution
	Pyridoxamine 5'-phosphate oxidase (EC 1.4.3.5)		1,082,657	S -> T	Substitution
	IS110 family transposase		701,051-702,610		Complete deletion

Table 3.2 Genes mutated in 1457 biofilm mutants

Mutant	Product	GenBank gene	Mutation location	Amino Acid Change	Protein Effect
PV18	ferrous iron transporter B	*feoB*	126,190	I -> T	Substitution
	phosphoenolpyruvate synthase regulatory protein		352,440	T -> C	Substitution
	intergenic region between Fst family toxin (type 1 TA system) and a hypothetical protein		582,168		
	19 bases from start codon of hypothetical protein		2,422,119		
	hypothetical protein		2,422,152-2,422,331		Multiple SNPs
	intergenic region between two hypothetical proteins		2,422,363-2,422,510		Multiple SNPs
PV19	intergenic		55,414-55,477		Multiple SNPs
	ferrous iron transporter B	*feoB*	126,190	I->T	Substitution
	Ybbr-like domain containing protein		753,490	G -> T	Truncation
	SigB	*sigB*	831,846	R->L	Substitution
	intergenic region between serine recombinase and glutathione-dependent formaldehyde dehydrogenase		1,855,652-1,855,744		Multiple SNPs
	intergenic region between Fst family toxin (type 1 TA system) and a hypothetical protein		2,421,830-2,422,087		Multiple SNPs
	19 bases from start codon of hypothetical protein		2,422,119		
	hypothetical protein		2,422,152-2,422,328		Multiple SNPs
	intergenic region between two hypothetical proteins		2,422,331-2,422,562		Multiple SNPs
PV21	intergenic		55,439-55,447		Multiple SNPs
	ferrous iron transporter B	*feoB*	126,190	I -> T	Substitution
	hypothetical protein			L->F	Substitution
	ribonuclease Y	*rny*	1,543,414	C -> A	Substitution
	intergenic region between serine recombinase and glutathione-dependent formaldehyde dehydrogenase		1,855,733-1,855,744		Multiple SNPs
	intergenic region between Fst family toxin (type 1 TA system) and a hypothetical protein		2,421,796-2,421,911		Multiple SNPs
	hypothetical protein		2,422,125-2,422,328		Multiple SNPs
	intergenic region between two hypothetical proteins		2,422,331-2,422,510		Multiple SNPs
PV22	ferrous iron transporter B	*feoB*	126,190	I -> T	Substitution
	poly-beta-1,6 N-acetyl-D-glucosamine synthase	*icaA*	228,289	V->G	Substitution

	19 bases from start codon of hypothetical protein		2,422,119		
	hypothetical protein		2,422,152-2,422,328		Multiple SNPs
	intergenic region between two hypothetical proteins		2,422,401		
22R5	ferrous iron transporter B	*feoB*	126,190	I -> T	Substitution
	esterase family protein (tributyrin esterase)		290,978	T->R	Substitution
	hypothetical protein		300,119	L->F	Substitution
	intergenic region between serine recombinase and glutathione-dependent formaldehyde dehydrogenase		1,855,626-1,855,744		Multiple SNPs
	intergenic region between Fst family toxin (type 1 TA system) and a hypothetical protein		2,421,796-2,422,087		Multiple SNPs
	19 bases from start codon of hypothetical protein		2,422,119		
	hypothetical protein		2,422,152-2,422,328		Multiple SNPs
	intergenic region between two hypothetical proteins		2,422,331-2,422,562		Multiple SNPs
	intergenic		2,422,585-2,422,607		Multiple SNPs
22R6	ferrous iron transporter B	*feoB*	126,190	I -> T	Substitution
	Hypothetical protein		300,119	L->F	Substitution
	immediately 5' of hypothetical protein		2,422,087-2,422,119		Multiple SNPs
	hypothetical protein		2,422,272-2,422,328		Multiple SNPs
	intergenic region between two hypothetical proteins		2,422,363-2,422,466		Multiple SNPs

Next, the plasmid pBursa, carrying the *bursa aurealis* transposon, was transduced into the reporter strains already carrying pFA545 (transposase). After growth at a permissive temperature (30°C), cells carrying both plasmids were heat shocked at 47°C, plated on erm^{10}, and grown at 47°C for two days. Resulting colonies were patched on to cam^{10}, tet^{10}, and erm^{10} and, again, grown at 47°C to confirm transposition of *bursa aurealis* and loss of pBursa and pFA545. Regrettably, we were unable to cure the plasmids despite altering the incubation temperature and antibiotic concentration. This demonstrates the overall difficulty of cloning in *S. epidermidis* and suggests that the method used to perform transposon mutagenesis in *S. aureus* (170) cannot be used in *S. epidermidis.*

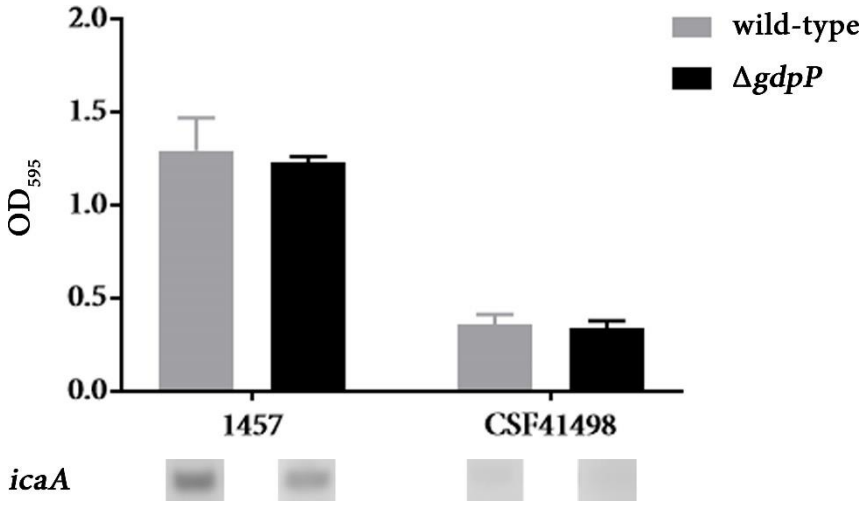

Figure 3.12. *gdpP* does not regulate *icaADBC*. 1457 was used to investigate whether phosphodiesterase contributed to the regulation of *icaADBC.* RNA extracted from mid-exponential phase of growth did not show a difference in *icaA* transcription level compared to wild-type in both 1457 and CSF41498 (A). PIA synthesis and biofilm formation also remained unchanged (A, B).

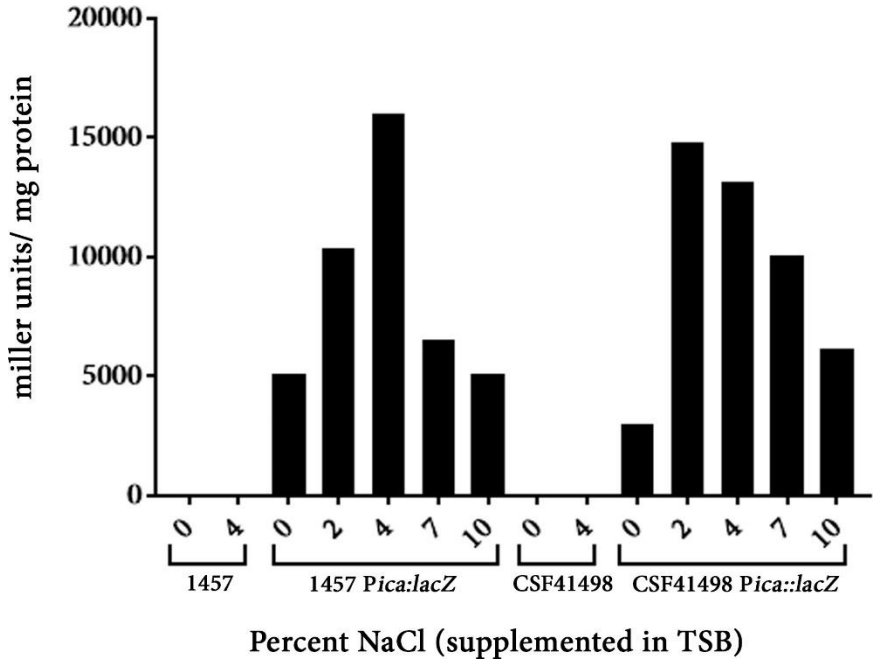

Figure 3.13. 2-4% NaCl is optimal for induction of *icaADBC* expression. *icaADBC* expression was determined based on *lacZ* expression as measured by β-galactosidase assay. 1457 P*ica*::*lacZ* and CSF41498 P*ica*::*lacZ* were grown in TSB with increasing concentrations of NaCl. 1457 and CSF41498 wild-types grown in TSB and 4% NaCl were included as negative controls.

CHAPTER 4

Discussion and concluding remarks

S. epidermidis is a commensal skin bacterium common on a variety of sites, including the nares, axillae, arms, and legs (171). As part of the skin microbiota, *S. epidermidis* has been shown to play a protective role by preventing colonization of pathogens (172, 173). However, *S. epidermidis* is also known to cause various infections and is the most frequent cause of those involving indwelling medical devices, including catheters, cerebral spinal fluid shunts, and prosthetic joints (174). Unlike the abundance of virulence factors that *S. aureus* possess, *S. epidermidis* has one major virulence factor which is the ability to form biofilms. While PIA has been shown to be an important component of biofilms, it is well known that not all *S. epidermidis* strains carry *icaADBC*, especially those isolated from healthy individuals (45, 64, 72, 90, 139-141). Furthermore, previous studies have shown that *ica* positive clinical isolates do not constitutively synthesize PIA (58, 90). These data suggest that PIA synthesis, while important during biofilm formation, is not always advantageous. Previously, our lab has reported that, in a skin colonization model, an *ica* mutant outcompetes the wild type strain that synthesizes high amounts of PIA. This, in combination with the observation that isolates from the skin of healthy individuals generally lack *icaADBC*, suggest that strains lacking this operon are selected for in this environment. One reason why this could be is that the presence of PIA is not beneficial on the skin surface and *S. epidermidis* utilizes other adhesive molecules for interaction with epithelial cells, such as the accumulation association protein (Aap). Additionally, the production of PIA occurs when the TCA cycle is inactive and requires channeling of carbon away from glycolysis. The synthesis of PIA requires a high energy investment so non-PIA producing isolates are selected for.

However, there are certain conditions in which PIA synthesis is important. Our lab has previously reported that *S. epidermidis* clinical isolates from a high shear environment (such as catheters) are more likely to carry the *ica* operon and synthesize PIA than those from low shear environments (90). Furthermore, *icaA* transcription and PIA synthesis is increased

when biofilms are grown under high shear flow (89, 90, 175). These data provide evidence that, while PIA is not advantageous under all conditions, there are circumstances under which strains able to synthesize high PIA are selected for. In this study, we utilized two *S. epidermidis* strains: 1457, isolated from a catheter infection (high shear) and synthesizes high PIA and biofilm (176), and CSF41498, isolated from a cerebral spinal fluid infection (low shear) and generally makes little PIA unless induced by NaCl (88). IcaR is a well characterized repressor of *icaADBC* (87, 88, 107-109, 112). However, 1457 Δ*icaR* did not have any observable effects on *icaA* transcription, PIA synthesis, or biofilm formation in 1457 but CSF41498 Δ*icaR* did. Transcriptional analysis of *icaR* showed that *icaR* transcription is lower in 1457 than in CSF41498 suggesting that IcaR does not regulate *icaADBC* in 1457 due to decreased *icaR* expression. Complementation of *icaR* using a constitutive promoter completely represses *icaA* transcription and PIA synthesis, demonstrating that IcaR is functional in 1457 and CSF41498.

Furthermore, in 1457, where *icaR* is not expressed, TcaR was shown to be the primary repressor as a *tcaR* mutant resulted in significantly increased *icaA* transcription, PIA synthesis, and biofilm formation. However, in CSF41498, where IcaR is expressed at high enough levels to sufficiently repress *icaADBC*, a *tcaR* mutant did not exhibit detectable levels of *icaA* transcription or PIA synthesis. This indicates that, when TcaR is absent, IcaR is capable of completely repressing *ica* transcription, even more than in wild-type. These data confirm previous reports that TcaR is not a major repressor of *icaADBC* (112) and only function when the primary repressor, IcaR, is not present. This suggests that TcaR may have a lower binding affinity than IcaR. To investigate this, we performed DNase I footprinting and, indeed, was able to show that both IcaR and TcaR bound to the intergenic region between *icaR* and *icaA.* While IcaR bound to one sequence near the *icaA* start site, TcaR bound to multiple sites. Chang et al. found that TcaR binds to a 33-bp pseudopalindromic sequence containing the consensus

sequence TTNNAA (111) although our footprinting data indicates the three sites are slightly shifted from the reported ones. One footprint does appear to overlap the IcaR binding site, suggesting that IcaR and TcaR could compete for binding to the *ica* promoter however, further experiments are required to confirm this. One method would be to perform additional EMSAs. As evident from our EMSA result, the binding of IcaR and TcaR to DNA cause different shifts in the migration of the DNA through the gel. This occurs because IcaR was reported to bind to DNA as two dimers while TcaR bound as a heptamer (108, 157). Based on this, if both IcaR and TcaR are added to the DNA at once, we would be able to determine which protein is binding based on the size of the shift. Additionally, if we can successfully generate IcaR- and TcaR-specific antibodies, western blot analysis of EMSAs would confirm which protein was binding to the DNA in a competition experiment.

Additionally, DNase footprinting assay showed that TcaR has binding sites in the *icaR* promoter confirming transcriptional data that TcaR can repress *icaR*. This indicates that TcaR can function as both a regulator of *icaR* and *icaADBC*, providing multiple ways in which TcaR can influence *icaADBC* transcription.

Our data, thus far, suggest that high PIA producing strains, such as 1457, have gained mutations leading to decreased *icaR* expression and de-rerepressed *icaADBC*. In an effort to identify these mutations, we sequenced 1457 mutants with decreased PIA synthesis and observed that, indeed, *icaR* transcription is higher. We were also able to easily isolate CSF41498 biofilm mutants displaying increased *icaA* transcription, PIA synthesis, and biofilm formation. Whole genome sequencing of these mutants revealed that each mutant contained single-nucleotide polymorphisms (SNPs) in multiple genes, suggesting that altered regulation of *icaR* could be due to mutations in multiple genes. Overall, this experiment demonstrate the level of regulation that *icaADBC* is subjected to and how mutants are selected for that allow it to be successful in different environments.

As an alternative to isolating biofilm mutants, we also attempted to perform a more direct method of identifying *icaADBC* regulators. This method involved using the transposon *bursa aurealis* to generate a library of mutants in P*ica::lacZ* reporters. The reporter will allow us to determine expression level of *icaADBC* in response to mutations in non-essential genes of *S. epidermidis.* Because transposon mutagenesis has already been successfully performed in *S. aureus* to generate the Nebraska Transposon Mutagenesis Library (177), we were confident that we could adapt this method to *S. epidermidis* due to the similarity in genetic manipulation between *S. aureus* and *S. epidermidis*. Unfortunately, we were unable to cure the plasmids pBursa and pFA545 despite multiple attempts with various conditions. While the method for genetic manipulation is the same, it is harder to make mutants in *S. epidermidis* and this is likely due to the difficulty in curing plasmids. Since generating mutations is not easy in *S. epidermidis*, it would be useful to have a library of mutants at hand. However, in order to achieve this, further work must be performed to develop a method capable of transposon mutagenesis as well as successful curing of the plasmids.

In this study, we sought out to further understand the regulation of *icaADBC* and PIA synthesis in *S. epidermidis.* Many investigators have observed that the presence of the *ica* operon and PIA synthesis are highly variable in *S. epidermidis* clinical isolates. Therefore, the objective of this study was to investigate the regulation of *icaADBC* with the hypothesis that, in *S. epidermidis, icaADBC* regulation, and therefore PIA synthesis, is variable due to dysregulation of *icaR* and *tcaR*, which encode for two repressors of the operon.

While PIA is one of the better understood biofilm components, there is still much to learn. While we were able to provide new insight into the regulation of *icaADBC* by IcaR and TcaR, we also uncovered new questions about how regulation may differ in each clinical isolate. The complexity of *icaADBC* regulation is reflective of its importance, not only as an adhesive molecule but the role it plays in disease progression as well as immune evasion. The

idea that *S. epidermidis* mutants can be selected for to adapt to different environments show the role of PIA in adaptation to various niches. Our results suggest that regulation of *icaADBC* is fairly complex as we identified multiple mutations that lead to altered PIA synthesis and biofilm formation.

CHAPTER 5

References cited

1. O'Gara JP, Humphreys H. 2001. Staphylococcus epidermidis biofilms: importance and implications. Journal of medical microbiology 50:582-587.
2. Gill SR, Fouts DE, Archer GL, Mongodin EF, Deboy RT, Ravel J, Paulsen IT, Kolonay JF, Brinkac L, Beanan M, Dodson RJ, Daugherty SC, Madupu R, Angiuoli SV, Durkin AS, Haft DH, Vamathevan J, Khouri H, Utterback T, Lee C, Dimitrov G, Jiang L, Qin H, Weidman J, Tran K, Kang K, Hance IR, Nelson KE, Fraser CM. 2005. Insights on evolution of virulence and resistance from the complete genome analysis of an early methicillin-resistant Staphylococcus aureus strain and a biofilm-producing methicillin-resistant Staphylococcus epidermidis strain. J Bacteriol 187:2426-38.
3. Cheng AG, Kim HK, Burts ML, Krausz T, Schneewind O, Missiakas DM. 2009. Genetic requirements for Staphylococcus aureus abscess formation and persistence in host tissues. FASEB J 23:3393-404.
4. Hecker M, Mader U, Volker U. 2018. From the genome sequence via the proteome to cell physiology - Pathoproteomics and pathophysiology of Staphylococcus aureus. Int J Med Microbiol doi:10.1016/j.ijmm.2018.01.002.
5. Stewart PS. 2002. Mechanisms of antibiotic resistance in bacterial biofilms. International journal of medical microbiology : IJMM 292:107-113.
6. Stewart PS, Costerton JW. 2001. Antibiotic resistance of bacteria in biofilms. Lancet (London, England) 358:135-138.
7. Darouiche RO. 2004. Treatment of infections associated with surgical implants. N Engl J Med 350:1422-9.
8. Wu H, Moser C, Wang HZ, Hoiby N, Song ZJ. 2015. Strategies for combating bacterial biofilm infections. Int J Oral Sci 7:1-7.

9. Heilmann C, Hussain M, Peters G, Gotz F. 1997. Evidence for autolysin-mediated primary attachment of Staphylococcus epidermidis to a polystyrene surface. Mol Microbiol 24:1013-24.

10. Clarke SR, Foster SJ. 2006. Surface adhesins of Staphylococcus aureus. Adv Microb Physiol 51:187-224.

11. Pei L, Flock JI. 2001. Lack of fbe, the gene for a fibrinogen-binding protein from Staphylococcus epidermidis, reduces its adherence to fibrinogen coated surfaces. Microb Pathog 31:185-93.

12. Pei L, Flock JI. 2001. Functional study of antibodies against a fibrogenin-binding protein in Staphylococcus epidermidis adherence to polyethylene catheters. J Infect Dis 184:52-5.

13. Sellman BR, Timofeyeva Y, Nanra J, Scott A, Fulginiti JP, Matsuka YV, Baker SM. 2008. Expression of Staphylococcus epidermidis SdrG increases following exposure to an in vivo environment. Infect Immun 76:2950-7.

14. Brennan MP, Loughman A, Devocelle M, Arasu S, Chubb AJ, Foster TJ, Cox D. 2009. Elucidating the role of Staphylococcus epidermidis serine-aspartate repeat protein G in platelet activation. J Thromb Haemost 7:1364-72.

15. Arrecubieta C, Lee MH, Macey A, Foster TJ, Lowy FD. 2007. SdrF, a Staphylococcus epidermidis surface protein, binds type I collagen. J Biol Chem 282:18767-76.

16. Arrecubieta C, Toba FA, von Bayern M, Akashi H, Deng MC, Naka Y, Lowy FD. 2009. SdrF, a Staphylococcus epidermidis surface protein, contributes to the initiation of ventricular assist device driveline-related infections. PLoS Pathog 5:e1000411.

17. Clarke SR, Harris LG, Richards RG, Foster SJ. 2002. Analysis of Ebh, a 1.1-megadalton cell wall-associated fibronectin-binding protein of Staphylococcus aureus. Infect Immun 70:6680-7.

18. Shahrooei M, Hira V, Stijlemans B, Merckx R, Hermans PW, Van Eldere J. 2009. Inhibition of Staphylococcus epidermidis biofilm formation by rabbit polyclonal antibodies against the SesC protein. Infect Immun 77:3670-8.

19. Sutherland I. 2001. Biofilm exopolysaccharides: a strong and sticky framework. Microbiology (Reading, England) 147:3-9.

20. Sutherland IW. 2001. The biofilm matrix--an immobilized but dynamic microbial environment. Trends in microbiology 9:222-227.

21. Vu B, Chen M, Crawford RJ, Ivanova EP. 2009. Bacterial extracellular polysaccharides involved in biofilm formation. Molecules (Basel, Switzerland) 14:2535-2554.

22. Branda SS, Vik S, Friedman L, Kolter R. 2005. Biofilms: the matrix revisited. Trends in microbiology 13:20-26.

23. Mack D, Fischer W, Krokotsch A, Leopold K, Hartmann R, Egge H, Laufs R. 1996. The intercellular adhesin involved in biofilm accumulation of Staphylococcus epidermidis is a linear beta-1,6-linked glucosaminoglycan: purification and structural analysis. Journal of Bacteriology 178:175-183.

24. Joo HS, Otto M. 2012. Molecular basis of in vivo biofilm formation by bacterial pathogens. Chemistry & biology 19:1503-1513.

25. O'Toole G, Kaplan HB, Kolter R. 2000. Biofilm formation as microbial development. Annual Review of Microbiology 54:49-79.

26. Otto M. 2008. Staphylococcal biofilms. Current topics in microbiology and immunology 322:207-228.

27. Moormeier DE, Bose JL, Horswill AR, Bayles KW. 2014. Temporal and stochastic control of Staphylococcus aureus biofilm development. mBio 5:e01341-14.

28. Otto M. 2013. Staphylococcal infections: mechanisms of biofilm maturation and detachment as critical determinants of pathogenicity. Annual Review of Medicine 64:175-188.

29. Otto M. 2009. Staphylococcus epidermidis--the 'accidental' pathogen. Nat Rev Microbiol 7:555-67.

30. Boles BR, Horswill AR. 2008. Agr-mediated dispersal of Staphylococcus aureus biofilms. PLoS pathogens 4:e1000052.

31. Mann EE, Rice KC, Boles BR, Endres JL, Ranjit D, Chandramohan L, Tsang LH, Smeltzer MS, Horswill AR, Bayles KW. 2009. Modulation of eDNA release and degradation affects Staphylococcus aureus biofilm maturation. PloS one 4:e5822.

32. Sharma-Kuinkel BK, Mann EE, Ahn JS, Kuechenmeister LJ, Dunman PM, Bayles KW. 2009. The Staphylococcus aureus LytSR two-component regulatory system affects biofilm formation. Journal of Bacteriology 191:4767-4775.

33. Kiedrowski MR, Kavanaugh JS, Malone CL, Mootz JM, Voyich JM, Smeltzer MS, Bayles KW, Horswill AR. 2011. Nuclease modulates biofilm formation in community-associated methicillin-resistant Staphylococcus aureus. PloS one 6:e26714.

34. Beenken KE, Spencer H, Griffin LM, Smeltzer MS. 2012. Impact of extracellular nuclease production on the biofilm phenotype of Staphylococcus aureus under in vitro and in vivo conditions. Infection and immunity 80:1634-1638.

35. Wang R, Khan BA, Cheung GY, Bach TH, Jameson-Lee M, Kong KF, Queck SY, Otto M. 2011. Staphylococcus epidermidis surfactant peptides promote biofilm maturation and dissemination of biofilm-associated infection in mice. The Journal of clinical investigation 121:238-248.

36. Periasamy S, Joo HS, Duong AC, Bach TH, Tan VY, Chatterjee SS, Cheung GY, Otto M. 2012. How Staphylococcus aureus biofilms develop their characteristic structure.

Proceedings of the National Academy of Sciences of the United States of America 109:1281-1286.

37. Wang X, Preston JF, 3rd, Romeo T. 2004. The pgaABCD locus of Escherichia coli promotes the synthesis of a polysaccharide adhesin required for biofilm formation. Journal of Bacteriology 186:2724-2734.

38. Choi AH, Slamti L, Avci FY, Pier GB, Maira-Litran T. 2009. The pgaABCD locus of Acinetobacter baumannii encodes the production of poly-beta-1-6-N-acetylglucosamine, which is critical for biofilm formation. Journal of Bacteriology 191:5953-5963.

39. Sloan GP, Love CF, Sukumar N, Mishra M, Deora R. 2007. The Bordetella Bps polysaccharide is critical for biofilm development in the mouse respiratory tract. Journal of Bacteriology 189:8270-8276.

40. Conover MS, Sloan GP, Love CF, Sukumar N, Deora R. 2010. The Bps polysaccharide of Bordetella pertussis promotes colonization and biofilm formation in the nose by functioning as an adhesin. Molecular microbiology 77:1439-1455.

41. Izano EA, Sadovskaya I, Vinogradov E, Mulks MH, Velliyagounder K, Ragunath C, Kher WB, Ramasubbu N, Jabbouri S, Perry MB, Kaplan JB. 2007. Poly-N-acetylglucosamine mediates biofilm formation and antibiotic resistance in Actinobacillus pleuropneumoniae. Microbial pathogenesis 43:1-9.

42. Jarrett CO, Deak E, Isherwood KE, Oyston PC, Fischer ER, Whitney AR, Kobayashi SD, DeLeo FR, Hinnebusch BJ. 2004. Transmission of Yersinia pestis from an infectious biofilm in the flea vector. The Journal of infectious diseases 190:783-792.

43. Yakandawala N, Gawande PV, LoVetri K, Cardona ST, Romeo T, Nitz M, Madhyastha S. 2011. Characterization of the poly-beta-1,6-N-acetylglucosamine polysaccharide

component of Burkholderia biofilms. Applied and Environmental Microbiology 77:8303-8309.

44. Cywes-Bentley C, Skurnik D, Zaidi T, Roux D, Deoliveira RB, Garrett WS, Lu X, O'Malley J, Kinzel K, Zaidi T, Rey A, Perrin C, Fichorova RN, Kayatani AK, Maira-Litran T, Gening ML, Tsvetkov YE, Nifantiev NE, Bakaletz LO, Pelton SI, Golenbock DT, Pier GB. 2013. Antibody to a conserved antigenic target is protective against diverse prokaryotic and eukaryotic pathogens. Proceedings of the National Academy of Sciences of the United States of America 110:E2209-18.

45. Cafiso V, Bertuccio T, Santagati M, Campanile F, Amicosante G, Perilli MG, Selan L, Artini M, Nicoletti G, Stefani S. 2004. Presence of the ica operon in clinical isolates of Staphylococcus epidermidis and its role in biofilm production. Clinical microbiology and infection : the official publication of the European Society of Clinical Microbiology and Infectious Diseases 10:1081-1088.

46. Cramton SE, Gerke C, Schnell NF, Nichols WW, Gotz F. 1999. The intercellular adhesion (ica) locus is present in Staphylococcus aureus and is required for biofilm formation. Infection and immunity 67:5427-5433.

47. Cue D, Lei MG, Lee CY. 2012. Genetic regulation of the intercellular adhesion locus in staphylococci. Frontiers in cellular and infection microbiology 2:38.

48. Fey PD, Olson ME. 2010. Current concepts in biofilm formation of Staphylococcus epidermidis. Future microbiology 5:917-933.

49. Gerke C, Kraft A, Sussmuth R, Schweitzer O, Gotz F. 1998. Characterization of the N-acetylglucosaminyltransferase activity involved in the biosynthesis of the Staphylococcus epidermidis polysaccharide intercellular adhesin. The Journal of biological chemistry 273:18586-18593.

50. Heilmann C, Schweitzer O, Gerke C, Vanittanakom N, Mack D, Gotz F. 1996. Molecular basis of intercellular adhesion in the biofilm-forming Staphylococcus epidermidis. Molecular microbiology 20:1083-1091.

51. Izano EA, Amarante MA, Kher WB, Kaplan JB. 2008. Differential roles of poly-N-acetylglucosamine surface polysaccharide and extracellular DNA in Staphylococcus aureus and Staphylococcus epidermidis biofilms. Appl Environ Microbiol 74:470-6.

52. Li H, Xu L, Wang J, Wen Y, Vuong C, Otto M, Gao Q. 2005. Conversion of Staphylococcus epidermidis strains from commensal to invasive by expression of the ica locus encoding production of biofilm exopolysaccharide. Infection and immunity 73:3188-3191.

53. Little DJ, Bamford NC, Pokrovskaya V, Robinson H, Nitz M, Howell PL. 2014. Structural basis for the De-N-acetylation of Poly-beta-1,6-N-acetyl-D-glucosamine in Gram-positive bacteria. The Journal of biological chemistry 289:35907-35917.

54. Mack D, Haeder M, Siemssen N, Laufs R. 1996. Association of biofilm production of coagulase-negative staphylococci with expression of a specific polysaccharide intercellular adhesin. The Journal of infectious diseases 174:881-884.

55. McKenney D, Hubner J, Muller E, Wang Y, Goldmann DA, Pier GB. 1998. The ica locus of Staphylococcus epidermidis encodes production of the capsular polysaccharide/adhesin. Infection and immunity 66:4711-4720.

56. O'Gara JP. 2007. ica and beyond: biofilm mechanisms and regulation in Staphylococcus epidermidis and Staphylococcus aureus. FEMS Microbiol Lett 270:179-88.

57. Olson ME, Garvin KL, Fey PD, Rupp ME. 2006. Adherence of Staphylococcus epidermidis to biomaterials is augmented by PIA. Clinical orthopaedics and related research 451:21-24.

58. Rohde H, Burandt EC, Siemssen N, Frommelt L, Burdelski C, Wurster S, Scherpe S, Davies AP, Harris LG, Horstkotte MA, Knobloch JK, Ragunath C, Kaplan JB, Mack D. 2007. Polysaccharide intercellular adhesin or protein factors in biofilm accumulation of Staphylococcus epidermidis and Staphylococcus aureus isolated from prosthetic hip and knee joint infections. Biomaterials 28:1711-1720.

59. Rupp ME, Fey PD, Heilmann C, Gotz F. 2001. Characterization of the importance of Staphylococcus epidermidis autolysin and polysaccharide intercellular adhesin in the pathogenesis of intravascular catheter-associated infection in a rat model. The Journal of infectious diseases 183:1038-1042.

60. Rupp ME, Ulphani JS, Fey PD, Bartscht K, Mack D. 1999. Characterization of the importance of polysaccharide intercellular adhesin/hemagglutinin of Staphylococcus epidermidis in the pathogenesis of biomaterial-based infection in a mouse foreign body infection model. Infection and immunity 67:2627-2632.

61. Rupp ME, Ulphani JS, Fey PD, Mack D. 1999. Characterization of Staphylococcus epidermidis polysaccharide intercellular adhesin/hemagglutinin in the pathogenesis of intravascular catheter-associated infection in a rat model. Infection and immunity 67:2656-2659.

62. Vuong C, Kidder JB, Jacobson ER, Otto M, Proctor RA, Somerville GA. 2005. Staphylococcus epidermidis polysaccharide intercellular adhesin production significantly increases during tricarboxylic acid cycle stress. Journal of Bacteriology 187:2967-2973.

63. Vuong C, Voyich JM, Fischer ER, Braughton KR, Whitney AR, DeLeo FR, Otto M. 2004. Polysaccharide intercellular adhesin (PIA) protects Staphylococcus epidermidis against major components of the human innate immune system. Cellular microbiology 6:269-275.

64. Ziebuhr W, Heilmann C, Gotz F, Meyer P, Wilms K, Straube E, Hacker J. 1997. Detection of the intercellular adhesion gene cluster (ica) and phase variation in Staphylococcus epidermidis blood culture strains and mucosal isolates. Infection and immunity 65:890-896.

65. Heilmann C, Gerke C, Perdreau-Remington F, Gotz F. 1996. Characterization of Tn917 insertion mutants of Staphylococcus epidermidis affected in biofilm formation. Infect Immun 64:277-82.

66. Vuong C, Kocianova S, Voyich JM, Yao Y, Fischer ER, DeLeo FR, Otto M. 2004. A crucial role for exopolysaccharide modification in bacterial biofilm formation, immune evasion, and virulence. The Journal of biological chemistry 279:54881-54886.

67. Cerca N, Jefferson KK, Maira-Litran T, Pier DB, Kelly-Quintos C, Goldmann DA, Azeredo J, Pier GB. 2007. Molecular basis for preferential protective efficacy of antibodies directed to the poorly acetylated form of staphylococcal poly-N-acetyl-beta-(1-6)-glucosamine. Infect Immun 75:3406-13.

68. Atkin KE, MacDonald SJ, Brentnall AS, Potts JR, Thomas GH. 2014. A different path: revealing the function of staphylococcal proteins in biofilm formation. FEBS letters 588:1869-1872.

69. Cho SH, Naber K, Hacker J, Ziebuhr W. 2002. Detection of the icaADBC gene cluster and biofilm formation in Staphylococcus epidermidis isolates from catheter-related urinary tract infections. International journal of antimicrobial agents 19:570-575.

70. Galdbart JO, Allignet J, Tung HS, Ryden C, El Solh N. 2000. Screening for Staphylococcus epidermidis markers discriminating between skin-flora strains and those responsible for infections of joint prostheses. The Journal of infectious diseases 182:351-355.

71. Zhang YQ, Ren SX, Li HL, Wang YX, Fu G, Yang J, Qin ZQ, Miao YG, Wang WY, Chen RS, Shen Y, Chen Z, Yuan ZH, Zhao GP, Qu D, Danchin A, Wen YM. 2003. Genome-based analysis of virulence genes in a non-biofilm-forming Staphylococcus epidermidis strain (ATCC 12228). Mol Microbiol 49:1577-93.

72. Galdbart JO, Allignet J, Tung HS, Ryden C, El Solh N. 2000. Screening for Staphylococcus epidermidis markers discriminating between skin-flora strains and those responsible for infections of joint prostheses. J Infect Dis 182:351-5.

73. Kozitskaya S, Olson ME, Fey PD, Witte W, Ohlsen K, Ziebuhr W. 2005. Clonal analysis of Staphylococcus epidermidis isolates carrying or lacking biofilm-mediating genes by multilocus sequence typing. J Clin Microbiol 43:4751-7.

74. Nayak N, Satpathy G, Nag HL, Venkatesh P, Ramakrishnan S, Nag TC, Prasad S. 2011. Slime production is essential for the adherence of Staphylococcus epidermidis in implant-related infections. J Hosp Infect 77:153-6.

75. Foster TJ. 2005. Immune evasion by staphylococci. Nat Rev Microbiol 3:948-58.

76. Kristian SA, Birkenstock TA, Sauder U, Mack D, Gotz F, Landmann R. 2008. Biofilm formation induces C3a release and protects Staphylococcus epidermidis from IgG and complement deposition and from neutrophil-dependent killing. J Infect Dis 197:1028-35.

77. Johnson GM, Lee DA, Regelmann WE, Gray ED, Peters G, Quie PG. 1986. Interference with granulocyte function by Staphylococcus epidermidis slime. Infect Immun 54:13-20.

78. Rodgers J, Phillips F, Olliff C. 1994. The effects of extracellular slime from Staphylococcus epidermidis on phagocytic ingestion and killing. FEMS Immunol Med Microbiol 9:109-15.

79. Schommer NN, Christner M, Hentschke M, Ruckdeschel K, Aepfelbacher M, Rohde H. 2011. Staphylococcus epidermidis uses distinct mechanisms of biofilm formation to interfere with phagocytosis and activation of mouse macrophage-like cells 774A.1. Infection and immunity 79:2267-2276.

80. Maira-Litran T, Kropec A, Abeygunawardana C, Joyce J, Mark G, 3rd, Goldmann DA, Pier GB. 2002. Immunochemical properties of the staphylococcal poly-N-acetylglucosamine surface polysaccharide. Infect Immun 70:4433-40.

81. Maira-Litran T, Kropec A, Goldmann DA, Pier GB. 2005. Comparative opsonic and protective activities of Staphylococcus aureus conjugate vaccines containing native or deacetylated Staphylococcal Poly-N-acetyl-beta-(1-6)-glucosamine. Infect Immun 73:6752-62.

82. Cerca N, Jefferson KK, Oliveira R, Pier GB, Azeredo J. 2006. Comparative antibody-mediated phagocytosis of Staphylococcus epidermidis cells grown in a biofilm or in the planktonic state. Infect Immun 74:4849-55.

83. Vuong C, Voyich JM, Fischer ER, Braughton KR, Whitney AR, DeLeo FR, Otto M. 2004. Polysaccharide intercellular adhesin (PIA) protects Staphylococcus epidermidis against major components of the human innate immune system. Cell Microbiol 6:269-75.

84. Knobloch JK, Bartscht K, Sabottke A, Rohde H, Feucht HH, Mack D. 2001. Biofilm formation by Staphylococcus epidermidis depends on functional RsbU, an activator of the sigB operon: differential activation mechanisms due to ethanol and salt stress. Journal of Bacteriology 183:2624-2633.

85. Rachid S, Ohlsen K, Witte W, Hacker J, Ziebuhr W. 2000. Effect of subinhibitory antibiotic concentrations on polysaccharide intercellular adhesin expression in

biofilm-forming Staphylococcus epidermidis. Antimicrobial Agents and Chemotherapy 44:3357-3363.

86. Cramton SE, Ulrich M, Gotz F, Doring G. 2001. Anaerobic conditions induce expression of polysaccharide intercellular adhesin in Staphylococcus aureus and Staphylococcus epidermidis. Infection and immunity 69:4079-4085.

87. Conlon KM, Humphreys H, O'Gara JP. 2002. Regulation of icaR gene expression in Staphylococcus epidermidis. FEMS microbiology letters 216:171-177.

88. Conlon KM, Humphreys H, O'Gara JP. 2002. icaR encodes a transcriptional repressor involved in environmental regulation of ica operon expression and biofilm formation in Staphylococcus epidermidis. Journal of Bacteriology 184:4400-4408.

89. Weaver WM, Milisavljevic V, Miller JF, Di Carlo D. 2012. Fluid flow induces biofilm formation in Staphylococcus epidermidis polysaccharide intracellular adhesin-positive clinical isolates. Applied and Environmental Microbiology 78:5890-5896.

90. Schaeffer CR, Hoang TN, Sudbeck CM, Alawi M, Tolo IE, Robinson DA, Horswill AR, Rohde H, Fey PD. 2016. Versatility of Biofilm Matrix Molecules in Staphylococcus epidermidis Clinical Isolates and Importance of Polysaccharide Intercellular Adhesin Expression during High Shear Stress. mSphere 1:10.1128/mSphere.00165-16. eCollection 2016 Sep-Oct.

91. Sadykov MR, Olson ME, Halouska S, Zhu Y, Fey PD, Powers R, Somerville GA. 2008. Tricarboxylic acid cycle-dependent regulation of Staphylococcus epidermidis polysaccharide intercellular adhesin synthesis. Journal of Bacteriology 190:7621-7632.

92. Sadykov MR, Zhang B, Halouska S, Nelson JL, Kreimer LW, Zhu Y, Powers R, Somerville GA. 2010. Using NMR metabolomics to investigate tricarboxylic acid cycle-dependent

signal transduction in Staphylococcus epidermidis. The Journal of biological chemistry 285:36616-36624.

93. Sadykov MR, Hartmann T, Mattes TA, Hiatt M, Jann NJ, Zhu Y, Ledala N, Landmann R, Herrmann M, Rohde H, Bischoff M, Somerville GA. 2011. CcpA coordinates central metabolism and biofilm formation in Staphylococcus epidermidis. Microbiology 157:3458-68.

94. Bruckner R, Titgemeyer F. 2002. Carbon catabolite repression in bacteria: choice of the carbon source and autoregulatory limitation of sugar utilization. FEMS Microbiol Lett 209:141-8.

95. Sonenshein AL. 2007. Control of key metabolic intersections in Bacillus subtilis. Nat Rev Microbiol 5:917-27.

96. Warner JB, Lolkema JS. 2003. A Crh-specific function in carbon catabolite repression in Bacillus subtilis. FEMS Microbiol Lett 220:277-80.

97. Kullik II, Giachino P. 1997. The alternative sigma factor sigmaB in Staphylococcus aureus: regulation of the sigB operon in response to growth phase and heat shock. Archives of Microbiology 167:151-159.

98. Ferreira A, Gray M, Wiedmann M, Boor KJ. 2004. Comparative genomic analysis of the sigB operon in Listeria monocytogenes and in other Gram-positive bacteria. Current microbiology 48:39-46.

99. Gertz S, Engelmann S, Schmid R, Ziebandt AK, Tischer K, Scharf C, Hacker J, Hecker M. 2000. Characterization of the sigma(B) regulon in Staphylococcus aureus. Journal of Bacteriology 182:6983-6991.

100. van Schaik W, Abee T. 2005. The role of sigmaB in the stress response of Gram-positive bacteria -- targets for food preservation and safety. Current opinion in biotechnology 16:218-224.

101. Sahoo S, Verma RK, Suresh AK, Rao KK, Bellare J, Suraishkumar GK. 2003. Macro-level and genetic-level responses of Bacillus subtilis to shear stress. Biotechnology progress 19:1689-1696.

102. Miyazaki E, Chen JM, Ko C, Bishai WR. 1999. The Staphylococcus aureus rsbW (orf159) gene encodes an anti-sigma factor of SigB. Journal of Bacteriology 181:2846-2851.

103. Bischoff M, Dunman P, Kormanec J, Macapagal D, Murphy E, Mounts W, Berger-Bachi B, Projan S. 2004. Microarray-based analysis of the Staphylococcus aureus sigmaB regulon. Journal of Bacteriology 186:4085-4099.

104. Pane-Farre J, Jonas B, Forstner K, Engelmann S, Hecker M. 2006. The sigmaB regulon in Staphylococcus aureus and its regulation. International journal of medical microbiology : IJMM 296:237-258.

105. Knobloch JK, Jager S, Horstkotte MA, Rohde H, Mack D. 2004. RsbU-dependent regulation of Staphylococcus epidermidis biofilm formation is mediated via the alternative sigma factor sigmaB by repression of the negative regulator gene icaR. Infection and immunity 72:3838-3848.

106. Handke LD, Slater SR, Conlon KM, O'Donnell ST, Olson ME, Bryant KA, Rupp ME, O'Gara JP, Fey PD. 2007. SigmaB and SarA independently regulate polysaccharide intercellular adhesin production in Staphylococcus epidermidis. Canadian journal of microbiology 53:82-91.

107. Jefferson KK, Cramton SE, Gotz F, Pier GB. 2003. Identification of a 5-nucleotide sequence that controls expression of the ica locus in Staphylococcus aureus and characterization of the DNA-binding properties of IcaR. Molecular microbiology 48:889-899.

108. Jeng WY, Ko TP, Liu CI, Guo RT, Liu CL, Shr HL, Wang AH. 2008. Crystal structure of IcaR, a repressor of the TetR family implicated in biofilm formation in Staphylococcus epidermidis. Nucleic acids research 36:1567-1577.

109. Cerca N, Brooks JL, Jefferson KK. 2008. Regulation of the intercellular adhesin locus regulator (icaR) by SarA, sigmaB, and IcaR in Staphylococcus aureus. Journal of Bacteriology 190:6530-6533.

110. McCallum N, Bischoff M, Maki H, Wada A, Berger-Bachi B. 2004. TcaR, a putative MarR-like regulator of sarS expression. Journal of Bacteriology 186:2966-2972.

111. Chang YM, Jeng WY, Ko TP, Yeh YJ, Chen CK, Wang AH. 2010. Structural study of TcaR and its complexes with multiple antibiotics from Staphylococcus epidermidis. Proceedings of the National Academy of Sciences of the United States of America 107:8617-8622.

112. Jefferson KK, Pier DB, Goldmann DA, Pier GB. 2004. The teicoplanin-associated locus regulator (TcaR) and the intercellular adhesin locus regulator (IcaR) are transcriptional inhibitors of the ica locus in Staphylococcus aureus. Journal of Bacteriology 186:2449-2456.

113. Fan JR, Zhang HX, Mu YG, Zheng QC. 2017. Studying the recognition mechanism of TcaR and ssDNA using molecular dynamic simulations. J Mol Graph Model 80:67-75.

114. Heinrichs JH, Bayer MG, Cheung AL. 1996. Characterization of the sar locus and its interaction with agr in Staphylococcus aureus. J Bacteriol 178:418-23.

115. Olson ME, Todd DA, Schaeffer CR, Paharik AE, Van Dyke MJ, Buttner H, Dunman PM, Rohde H, Cech NB, Fey PD, Horswill AR. 2014. Staphylococcus epidermidis agr quorum-sensing system: signal identification, cross talk, and importance in colonization. J Bacteriol 196:3482-93.

116. Cheung AL, Zhang G. 2002. Global regulation of virulence determinants in Staphylococcus aureus by the SarA protein family. Front Biosci 7:d1825-42.

117. Valle J, Toledo-Arana A, Berasain C, Ghigo JM, Amorena B, Penades JR, Lasa I. 2003. SarA and not sigmaB is essential for biofilm development by Staphylococcus aureus. Mol Microbiol 48:1075-87.

118. Conlon KM, Humphreys H, O'Gara JP. 2004. Inactivations of rsbU and sarA by IS256 represent novel mechanisms of biofilm phenotypic variation in Staphylococcus epidermidis. J Bacteriol 186:6208-19.

119. Beenken KE, Blevins JS, Smeltzer MS. 2003. Mutation of sarA in Staphylococcus aureus limits biofilm formation. Infect Immun 71:4206-11.

120. Tormo MA, Marti M, Valle J, Manna AC, Cheung AL, Lasa I, Penades JR. 2005. SarA is an essential positive regulator of Staphylococcus epidermidis biofilm development. Journal of Bacteriology 187:2348-2356.

121. Jager S, Jonas B, Pfanzelt D, Horstkotte MA, Rohde H, Mack D, Knobloch JK. 2009. Regulation of biofilm formation by sigma B is a common mechanism in Staphylococcus epidermidis and is not mediated by transcriptional regulation of sarA. The International journal of artificial organs 32:584-591.

122. Cue D, Lei MG, Lee CY. 2013. Activation of sarX by Rbf is required for biofilm formation and icaADBC expression in Staphylococcus aureus. J Bacteriol 195:1515-24.

123. Cue D, Lei MG, Luong TT, Kuechenmeister L, Dunman PM, O'Donnell S, Rowe S, O'Gara JP, Lee CY. 2009. Rbf promotes biofilm formation by Staphylococcus aureus via repression of icaR, a negative regulator of icaADBC. Journal of Bacteriology 191:6363-6373.

124. Rowe SE, Mahon V, Smith SG, O'Gara JP. 2011. A novel role for SarX in Staphylococcus epidermidis biofilm regulation. Microbiology (Reading, England) 157:1042-1049.

125. Rowe SE, Campbell C, Lowry C, O'Donnell ST, Olson ME, Lindgren JK, Waters EM, Fey PD, O'Gara JP. 2016. AraC-Type Regulator Rbf Controls the Staphylococcus epidermidis Biofilm Phenotype by Negatively Regulating the icaADBC Repressor SarR. J Bacteriol 198:2914-2924.

126. Yarwood JM, McCormick JK, Schlievert PM. 2001. Identification of a novel two-component regulatory system that acts in global regulation of virulence factors of Staphylococcus aureus. J Bacteriol 183:1113-23.

127. Wu Y, Wu Y, Zhu T, Han H, Liu H, Xu T, Francois P, Fischer A, Bai L, Gotz F, Qu D. 2015. Staphylococcus epidermidis SrrAB regulates bacterial growth and biofilm formation differently under oxic and microaerobic conditions. J Bacteriol 197:459-76.

128. Meier S, Goerke C, Wolz C, Seidl K, Homerova D, Schulthess B, Kormanec J, Berger-Bachi B, Bischoff M. 2007. sigmaB and the sigmaB-dependent arlRS and yabJ-spoVG loci affect capsule formation in Staphylococcus aureus. Infect Immun 75:4562-71.

129. Fournier B, Klier A, Rapoport G. 2001. The two-component system ArlS-ArlR is a regulator of virulence gene expression in Staphylococcus aureus. Mol Microbiol 41:247-61.

130. Wu Y, Wang J, Xu T, Liu J, Yu W, Lou Q, Zhu T, He N, Ben H, Hu J, Gotz F, Qu D. 2012. The two-component signal transduction system ArlRS regulates Staphylococcus epidermidis biofilm formation in an ica-dependent manner. PloS one 7:e40041.

131. Majerczyk CD, Sadykov MR, Luong TT, Lee C, Somerville GA, Sonenshein AL. 2008. Staphylococcus aureus CodY negatively regulates virulence gene expression. J Bacteriol 190:2257-65.

132. Majerczyk CD, Dunman PM, Luong TT, Lee CY, Sadykov MR, Somerville GA, Bodi K, Sonenshein AL. 2010. Direct targets of CodY in Staphylococcus aureus. J Bacteriol 192:2861-77.

133. Schauder S, Shokat K, Surette MG, Bassler BL. 2001. The LuxS family of bacterial autoinducers: biosynthesis of a novel quorum-sensing signal molecule. Mol Microbiol 41:463-76.

134. Yu D, Zhao L, Xue T, Sun B. 2012. Staphylococcus aureus autoinducer-2 quorum sensing decreases biofilm formation in an icaR-dependent manner. BMC Microbiol 12:288.

135. Ma R, Qiu S, Jiang Q, Sun H, Xue T, Cai G, Sun B. 2017. AI-2 quorum sensing negatively regulates rbf expression and biofilm formation in Staphylococcus aureus. Int J Med Microbiol 307:257-267.

136. Xue T, Ni J, Shang F, Chen X, Zhang M. 2015. Autoinducer-2 increases biofilm formation via an ica- and bhp-dependent manner in Staphylococcus epidermidis RP62A. Microbes and infection / Institut Pasteur 17:345-352.

137. Nakano S, Kuster-Schock E, Grossman AD, Zuber P. 2003. Spx-dependent global transcriptional control is induced by thiol-specific oxidative stress in Bacillus subtilis. Proc Natl Acad Sci U S A 100:13603-8.

138. Pamp SJ, Frees D, Engelmann S, Hecker M, Ingmer H. 2006. Spx is a global effector impacting stress tolerance and biofilm formation in Staphylococcus aureus. J Bacteriol 188:4861-70.

139. Wojtyczka RD, Orlewska K, Kepa M, Idzik D, Dziedzic A, Mularz T, Krawczyk M, Miklasinska M, Wasik TJ. 2014. Biofilm formation and antimicrobial susceptibility of Staphylococcus epidermidis strains from a hospital environment. Int J Environ Res Public Health 11:4619-33.

140. Oliveira A, Cunha Mde L. 2010. Comparison of methods for the detection of biofilm production in coagulase-negative staphylococci. BMC Res Notes 3:260.

141. Arciola CR, Baldassarri L, Montanaro L. 2001. Presence of icaA and icaD genes and slime production in a collection of staphylococcal strains from catheter-associated infections. J Clin Microbiol 39:2151-6.

142. Brooks JL, Jefferson KK. 2014. Phase variation of poly-N-acetylglucosamine expression in Staphylococcus aureus. PLoS Pathog 10:e1004292.

143. Ziebuhr W, Krimmer V, Rachid S, Lossner I, Gotz F, Hacker J. 1999. A novel mechanism of phase variation of virulence in Staphylococcus epidermidis: evidence for control of the polysaccharide intercellular adhesin synthesis by alternating insertion and excision of the insertion sequence element IS256. Mol Microbiol 32:345-56.

144. Deighton M, Pearson S, Capstick J, Spelman D, Borland R. 1992. Phenotypic variation of Staphylococcus epidermidis isolated from a patient with native valve endocarditis. J Clin Microbiol 30:2385-90.

145. Christensen GD, Baddour LM, Simpson WA. 1987. Phenotypic variation of Staphylococcus epidermidis slime production in vitro and in vivo. Infect Immun 55:2870-7.

146. Eftekhar F, Speert DP. 2009. Biofilm formation by persistent and non-persistent isolates of Staphylococcus epidermidis from a neonatal intensive care unit. J Hosp Infect 71:112-6.

147. Chokr A, Watier D, Eleaume H, Pangon B, Ghnassia JC, Mack D, Jabbouri S. 2006. Correlation between biofilm formation and production of polysaccharide intercellular adhesin in clinical isolates of coagulase-negative staphylococci. Int J Med Microbiol 296:381-8.

148. Schaeffer CR, Woods KM, Longo GM, Kiedrowski MR, Paharik AE, Buttner H, Christner M, Boissy RJ, Horswill AR, Rohde H, Fey PD. 2015. Accumulation-associated protein enhances Staphylococcus epidermidis biofilm formation under dynamic conditions

and is required for infection in a rat catheter model. Infection and immunity 83:214-226.

149. Mack D, Bartscht K, Fischer C, Rohde H, de Grahl C, Dobinsky S, Horstkotte MA, Kiel K, Knobloch JK. 2001. Genetic and biochemical analysis of Staphylococcus epidermidis biofilm accumulation. Methods Enzymol 336:215-39.

150. Winstel V, Kuhner P, Krismer B, Peschel A, Rohde H. 2015. Transfer of plasmid DNA to clinical coagulase-negative staphylococcal pathogens by using a unique bacteriophage. Appl Environ Microbiol 81:2481-8.

151. Olson ME, Horswill AR. 2014. Bacteriophage Transduction in Staphylococcus epidermidis. Methods Mol Biol 1106:167-72.

152. Augustin J, Gotz F. 1990. Transformation of Staphylococcus epidermidis and other staphylococcal species with plasmid DNA by electroporation. FEMS Microbiol Lett 54:203-7.

153. Kreiswirth BN, Lofdahl S, Betley MJ, O'Reilly M, Schlievert PM, Bergdoll MS, Novick RP. 1983. The toxic shock syndrome exotoxin structural gene is not detectably transmitted by a prophage. Nature 305:709-12.

154. Studier FW, Moffatt BA. 1986. Use of bacteriophage T7 RNA polymerase to direct selective high-level expression of cloned genes. Journal of Molecular Biology 189:113-130.

155. Waters EM, McCarthy H, Hogan S, Zapotoczna M, O'Neill E, O'Gara JP. 2014. Rapid quantitative and qualitative analysis of biofilm production by Staphylococcus epidermidis under static growth conditions. Methods Mol Biol 1106:157-66.

156. Snesrud E, Ong AC, Corey B, Kwak YI, Clifford R, Gleeson T, Wood S, Whitman TJ, Lesho EP, Hinkle M, Mc Gann P. 2017. Analysis of Serial Isolates of mcr-1- positive

Escherichia coli Reveals a Highly Active ISApl1 Transposon. Antimicrob Agents Chemother doi:10.1128/AAC.00056-17.

157. Chang YM, Ho CH, Chen CK, Maestre-Reyna M, Chang-Chien MW, Wang AH. 2014. TcaR-ssDNA complex crystal structure reveals new DNA binding mechanism of the MarR family proteins. Nucleic acids research 42:5314-5321.

158. Maki H, McCallum N, Bischoff M, Wada A, Berger-Bachi B. 2004. tcaA inactivation increases glycopeptide resistance in Staphylococcus aureus. Antimicrob Agents Chemother 48:1953-9.

159. Olson ME, Slater SR, Rupp ME, Fey PD. 2010. Rifampicin enhances activity of daptomycin and vancomycin against both a polysaccharide intercellular adhesin (PIA)-dependent and -independent Staphylococcus epidermidis biofilm. J Antimicrob Chemother 65:2164-71.

160. Serrano M, Zilhao R, Ricca E, Ozin AJ, Moran CP, Jr., Henriques AO. 1999. A Bacillus subtilis secreted protein with a role in endospore coat assembly and function. J Bacteriol 181:3632-43.

161. Hamon MA, Stanley NR, Britton RA, Grossman AD, Lazazzera BA. 2004. Identification of AbrB-regulated genes involved in biofilm formation by Bacillus subtilis. Mol Microbiol 52:847-60.

162. Ruiz de los Mozos I, Vergara-Irigaray M, Segura V, Villanueva M, Bitarte N, Saramago M, Domingues S, Arraiano CM, Fechter P, Romby P, Valle J, Solano C, Lasa I, Toledo-Arana A. 2013. Base pairing interaction between 5'- and 3'-UTRs controls icaR mRNA translation in Staphylococcus aureus. PLoS Genet 9:e1004001.

163. Ryjenkov DA, Tarutina M, Moskvin OV, Gomelsky M. 2005. Cyclic diguanylate is a ubiquitous signaling molecule in bacteria: insights into biochemistry of the GGDEF protein domain. J Bacteriol 187:1792-8.

164. Sasakura Y, Hirata S, Sugiyama S, Suzuki S, Taguchi S, Watanabe M, Matsui T, Sagami I, Shimizu T. 2002. Characterization of a direct oxygen sensor heme protein from Escherichia coli. Effects of the heme redox states and mutations at the heme-binding site on catalysis and structure. J Biol Chem 277:23821-7.

165. Holland LM, O'Donnell ST, Ryjenkov DA, Gomelsky L, Slater SR, Fey PD, Gomelsky M, O'Gara JP. 2008. A staphylococcal GGDEF domain protein regulates biofilm formation independently of cyclic dimeric GMP. J Bacteriol 190:5178-89.

166. Du B, Ji W, An H, Shi Y, Huang Q, Cheng Y, Fu Q, Wang H, Yan Y, Sun J. 2014. Functional analysis of c-di-AMP phosphodiesterase, GdpP, in Streptococcus suis serotype 2. Microbiol Res 169:749-58.

167. Corrigan RM, Abbott JC, Burhenne H, Kaever V, Grundling A. 2011. c-di-AMP is a new second messenger in Staphylococcus aureus with a role in controlling cell size and envelope stress. PLoS Pathog 7:e1002217.

168. Peng X, Zhang Y, Bai G, Zhou X, Wu H. 2016. Cyclic di-AMP mediates biofilm formation. Mol Microbiol 99:945-59.

169. Townsley L, Yannarell SM, Huynh TN, Woodward JJ, Shank EA. 2018. Cyclic di-AMP Acts as an Extracellular Signal That Impacts Bacillus subtilis Biofilm Formation and Plant Attachment. MBio 9.

170. Yajjala VK, Widhelm TJ, Endres JL, Fey PD, Bayles KW. 2016. Generation of a Transposon Mutant Library in Staphylococcus aureus and Staphylococcus epidermidis Using bursa aurealis. Methods Mol Biol 1373:103-10.

171. Kloos WE, Musselwhite MS. 1975. Distribution and persistence of Staphylococcus and Micrococcus species and other aerobic bacteria on human skin. Applied Microbiology 30:381-385.

172. Cogen A, Nizet V, Gallo R. Staphylococcus epidermidis functions as a component of the skin innate immune system by inhibiting the pathogen Group A Streptococcus, p S131-S131. *In* (ed), Nature Publishing Group 75 Varick Street, 9th Floor, New York, NY 10013-1917 USA,

173. Cogen AL, Nizet V, Gallo RL. 2008. Skin microbiota: a source of disease or defence? Br J Dermatol 158:442-55.

174. Rogers KL, Fey PD, Rupp ME. 2009. Coagulase-negative staphylococcal infections. Infectious disease clinics of North America 23:73-98.

175. Foka A, Katsikogianni MG, Anastassiou ED, Spiliopoulou I, Missirlis YF. 2012. The combined effect of surface chemistry and flow conditions on Staphylococcus epidermidis adhesion and ica operon expression. European cells & materials 24:386-402.

176. Mack D, Siemssen N, Laufs R. 1992. Parallel induction by glucose of adherence and a polysaccharide antigen specific for plastic-adherent Staphylococcus epidermidis: evidence for functional relation to intercellular adhesion. Infect Immun 60:2048-57.

177. Fey PD, Endres JL, Yajjala VK, Widhelm TJ, Boissy RJ, Bose JL, Bayles KW. 2013. A genetic resource for rapid and comprehensive phenotype screening of nonessential Staphylococcus aureus genes. mBio 4:e00537-12.